

January 2012

Cell Adhesion and Migration on NDGA Cross-Linked Fibrillar Collagen Matrices for Tendon Tissue Engineering

Ana Ysabel Rioja

University of South Florida, anayrioja@gmail.com

Follow this and additional works at: <http://scholarcommons.usf.edu/etd>



Part of the [American Studies Commons](#), and the [Biomedical Engineering and Bioengineering Commons](#)

Scholar Commons Citation

Rioja, Ana Ysabel, "Cell Adhesion and Migration on NDGA Cross-Linked Fibrillar Collagen Matrices for Tendon Tissue Engineering" (2012). *Graduate Theses and Dissertations*.
<http://scholarcommons.usf.edu/etd/4214>

This Thesis is brought to you for free and open access by the Graduate School at Scholar Commons. It has been accepted for inclusion in Graduate Theses and Dissertations by an authorized administrator of Scholar Commons. For more information, please contact scholarcommons@usf.edu.

Cell Adhesion and Migration on NDGA Cross-Linked Fibrillar Collagen Matrices
for Tendon Tissue Engineering

by

Ana Ysabel Rioja

A thesis submitted in partial fulfillment
of the requirements for the degree of
Master of Science in Biomedical Engineering
Department of Chemical and Biomedical Engineering
College of Engineering
University of South Florida

Co-Major Professor: Nathan D. Gallant, Ph.D.

Co-Major Professor: Thomas J. Koob, Ph.D.

Mark Jaroszeski, Ph.D.

Piyush Koria, Ph.D.

Date of Approval:

June 7, 2012

Keywords: biomaterials, cell adhesion strength, cell morphology, di-catechol
nordihydroguaiaretic acid, fibroblasts

Copyright © 2012, Ana Ysabel Rioja

DEDICATION

This thesis is dedicated to my parents Jesus H. Rioja and Ruby Y. Sanchez and my sister Paola E. Rioja. Thank you for believing that I could accomplish anything I set my mind to. I especially want to thank my parents who spend all their time and effort helping me accomplish my dreams. I would not be who I am without both of you and I know I will never be able to finish thanking you for all your dedication and guidance.

ACKNOWLEDGMENTS

I would like to thank my advisors, Dr. Nathan D. Gallant and Dr. Thomas J. Koob, for allowing me to work on a new and fascinating project where I had the opportunity to gain knowledge of various research techniques. I would also like to thank Dr. Mark Jaroszeski, and Dr. Piyush Koria for taking time to be part of my committee, Mr. Bernard Batson for supporting me through my undergraduate and graduate career at USF and introducing me to many wonderful people who have helped me all these years, Yvonne Davis for introducing me to the research world, the Nanotechnology Research & Education center staff for helping me with thickness measurements, and all my lab mates for their support.

I would especially like to thank Dr. Gallant for allowing me to be part of his research group and for believing in me. Thanks to his guidance and support I gained scientific qualities that I know will help me in my future career. I am also very thankful to God for giving me many blessings and wonderful parents who have supported me during my entire education.

TABLE OF CONTENTS

| | |
|---|-----|
| LIST OF FIGURES | iii |
| ABSTRACT..... | v |
| CHAPTER 1: INTRODUCTION..... | 1 |
| 1.1 Tendons..... | 1 |
| 1.2 Tendon Healing Process | 3 |
| 1.3 Tendon Healing Techniques | 4 |
| 1.3.1 Suturing Techniques | 5 |
| 1.4 Materials for Tendon Healing..... | 6 |
| 1.4.1 Tissue Grafts | 6 |
| 1.4.2 Synthetic Materials | 7 |
| 1.4.3 Other Biomaterials..... | 9 |
| 1.5 Collagen..... | 10 |
| 1.5.1 Collagen Type I..... | 12 |
| 1.5.2 Utilization of Collagen in Biomedical Applications..... | 13 |
| 1.5.2.1 Collagen Fibers | 13 |
| 1.5.2.2 Reconstructive Fibrils | 14 |
| 1.6 Collagen Fixation Methods..... | 15 |
| 1.6.1 Glutaraldehyde Treatment | 16 |
| 1.6.2 Carbodiimide Treatment | 17 |
| 1.6.3 NDGA Treatment..... | 18 |
| 1.7 Adhesion Assays..... | 21 |
| 1.7.1 Centrifugation | 22 |
| 1.7.2 Micromanipulation..... | 22 |
| 1.7.3 Hydrodynamic Shear Assay..... | 23 |
| 1.7.3.1 Parallel Plates..... | 23 |
| 1.7.3.2 Spinning Disk..... | 24 |
| 1.8 Migration Assays | 26 |
| 1.8.1 Wound Healing Assay | 28 |
| 1.8.2 Compartmentalization Techniques | 29 |
| 1.9 Thesis Objectives | 30 |
| CHAPTER 2: MATERIALS AND METHODS | 31 |
| 2.1 Cell Culture Reagents | 31 |
| 2.2 Collagen Gel and Film Preparation..... | 31 |
| 2.3 NDGA Cross-Linking..... | 34 |
| 2.3.1 Films - NDGA Treatment | 34 |

| | |
|--|--------------|
| 2.3.2 Gels - NDGA Treatment..... | 36 |
| 2.4 Absorbance of Collagen Networks..... | 37 |
| 2.5 Gel and Film Thickness Measurements..... | 38 |
| 2.5.1 Thickness Measurements Using Contact Angle Software..... | 38 |
| 2.5.2 Contact Profiler Measurements..... | 40 |
| 2.5.3 Optical Profiler Measurements..... | 42 |
| 2.6 Cell Adhesion Strength Experiments..... | 43 |
| 2.7 Cell Spreading Area and Morphology..... | 46 |
| 2.8 Cell Migration Experiments..... | 46 |
| CHAPTER 3: RESULTS..... | 49 |
| 3.1 Optical Density (O.D.) vs. Wavelength of Collagen Networks..... | 49 |
| 3.2 Collagen Gel/Film Thickness Measurements..... | 50 |
| 3.3 Cell Adhesion Strength Experiments..... | 52 |
| 3.3.1 Temporal Studies of Adhesion Strength..... | 52 |
| 3.3.2 Comparison of Adhesion Strength between <i>Wet</i> Gels, <i>Dry</i> , Native, and Cross-Linked Films..... | 54 |
| 3.4 Spreading/Circularity Experiments..... | 55 |
| 3.4.1 Temporal Cell Spreading Studies on Cross-Linked and Native <i>Wet</i> Collagen Gels..... | 56 |
| 3.4.2 Temporal Cell Circularity Studies on Cross-Linked and Native <i>Wet</i> Collagen Gels..... | 57 |
| 3.4.3 Temporal Cell Spreading Studies on Cross-Linked and Native <i>Re-hydrated</i> Collagen Films..... | 58 |
| 3.4.4 Temporal Cell Circularity Studies on Cross-Linked and Native <i>Re-hydrated</i> Collagen Films..... | 60 |
| 3.5 Cell Migration Experiments..... | 62 |
| CHAPTER 4: DISCUSSION..... | 65 |
| CHAPTER 5: CONCLUSIONS AND FUTURE WORK..... | 74 |
| REFERENCES..... | 78 |
| APPENDICES..... | 85 |
| Appendix A: Copyright Permissions..... | 86 |
| ABOUT THE AUTHOR..... | END PAGE |

LIST OF FIGURES

| | |
|--|----|
| Figure 1 The Achilles tendon (Gray, 1918 - public domain)..... | 2 |
| Figure 2 Collagen fiber formation | 12 |
| Figure 3 Glutaraldehyde cross-linked collagen. | 17 |
| Figure 4 Chemical structure of 1-ethyl-3-(3-dimethylaminopropyl)carbodiimide (EDC). | 18 |
| Figure 5 Diagram of NDGA molecule..... | 19 |
| Figure 6 Properties of 5% gelatin gels with different NDGA concentrations | 20 |
| Figure 7 Spinning disk device and radial/shear stress relation (an increase in the radius (r) is related to a linear increase in shear stress (τ))..... | 24 |
| Figure 8 The adhesion profile of a typical cell adhesion curve | 25 |
| Figure 9 Activation of glass cover slips with amine groups..... | 32 |
| Figure 10 Rinsing of 800 μ L collagen gels with deionized water | 33 |
| Figure 11 <i>Wet</i> collagen gels (800 μ L) left to dry overnight to form films | 33 |
| Figure 12 NDGA cross-linking of 800 μ L collagen films..... | 35 |
| Figure 13 <i>Dry</i> NDGA cross-linked collagen films (800 μ L) left to dry overnight..... | 36 |
| Figure 14 Synergy HT multi-mode microplate reader (Biotek Instruments, Inc). | 37 |
| Figure 15 Images taken with contact angle software- Part I..... | 38 |
| Figure 16 Images taken with contact angle software- Part II. | 39 |
| Figure 17 Image of 800 μ L <i>dry</i> collagen film using the contact angle software | 40 |
| Figure 18 Graph of thickness of 800 μ L <i>dry</i> collagen gel using contact profiler (x-axis: micrometer, y-axis: Angstrom)..... | 41 |

| | |
|--|----|
| Figure 19 Three dimensional interactive display of collagen - glass border with optical profiler | 42 |
| Figure 20 X-profile graph of thickness of 800 μ L <i>dry</i> collagen film using optical profiler | 43 |
| Figure 21 Diagram of spinning disk device | 43 |
| Figure 22 Stitching image of fibroblasts on a <i>wet</i> cross-linked surface taken immediately after fence removal | 47 |
| Figure 23 Absorbance of native and cross-linked collagen networks | 49 |
| Figure 24 Thickness of collagen samples using different measuring techniques (N = 3). | 50 |
| Figure 25 Temporal studies of adhesion strength for NIH 3T3 on 200 μ L collagen gels (N \geq 4)..... | 53 |
| Figure 26 Temporal studies of adhesion strength for NIH 3T3 on 800 μ L collagen films (N \geq 4) | 54 |
| Figure 27 Adhesion data of fibroblast on <i>wet</i> (200 μ L) and <i>dry</i> (800 μ l) collagen gels (N \geq 6)..... | 55 |
| Figure 28 Cell spreading area of NIH 3T3 on 200 μ L uncross-linked and cross-linked <i>wet</i> collagen gels at 4hr and 24hr (N = 3). | 56 |
| Figure 29 Statistical analysis of cell spreading area on 200 μ L <i>wet</i> collagen gels | 57 |
| Figure 30 Cell circularity of NIH 3T3 on uncross-linked and cross-linked <i>wet</i> collagen gels at 4hr and 24hr..... | 58 |
| Figure 31 Cell spreading area of NIH 3T3 on 800 μ L uncross-linked and cross-linked <i>re-hydrated</i> collagen films at 4hr and 24hr (N = 3). | 59 |
| Figure 32 Statistical analysis of cell spreading area on 800 μ L <i>re-hydrated</i> collagen films. | 60 |
| Figure 33 Cell circularity of NIH 3T3 on 800 μ L uncross-linked and cross-linked <i>dry</i> collagen films at 4hr and 24hr..... | 61 |
| Figure 34 Analysis of 24 hours migration experiments (change in radius) with NIS Elements software..... | 62 |
| Figure 35 Average radial migration speed in 24 hours (N \geq 8) | 63 |

ABSTRACT

Tendons, essential tissues that connect muscles to bones, are susceptible to rupture/degeneration due to their continuous use for enabling movement. Often surgical intervention is required to repair the tendon; relieving the pain and fixing the limited mobility that occurs from the damage. Unfortunately, post-surgery immobilization techniques required to restore tendon properties frequently lead to scar formation and reduced tendon range of motion. Our ultimate goal is to create an optimal tendon prosthetic that can stabilize the damaged muscle-bone connection and then be remodeled by resident cells from the surrounding tissues over time to ensure long-term function. To achieve this, we must first understand how cells respond to and interact with candidate replacement materials.

The most abundant extracellular matrix (ECM) protein found in the body, collagen, is chosen as the replacement material because it makes up the majority of tendon dry mass and it can be remodeled by cell-based homeostatic processes. Previous studies found that Di-catechol nordihydroguaiaretic acid (NDGA) cross-linked fibers have greater mechanical strength than native tendons; and for this reason this biomaterial could be used for tendon replacement.

This work focuses on investigating the behavior of fibroblasts on NDGA cross-linked and uncross-linked collagen samples to determine if cross-linking disrupts the cell binding sites affecting cell spreading, attachment, and migration. The *in-vitro* platform

was designed by plasma treating 25 mm diameter cover slips that were exposed to 3-aminopropyl-trimethoxysilane/toluene and glutaraldehyde/ethanol solutions. The collagen solution was then dispensed onto the glutaraldehyde-coated cover slip and incubated for fibrillar collagen matrix formation. The collagen matrices were submerged in NDGA cross-linking solution for 24 hours to ensure the surface was completely cross-linked. Collagen films were made by allowing the uncross-linked gels to dry overnight before and after NDGA treatment, resulting in a more compacted structure.

A spinning disk device was employed to quantify the ability of cells to remain attached to the collagen samples when exposed to hydrodynamic forces. To avoid any cell-cell interaction and focus on cell-surface interactions, 50-100 cells/mm² were seeded carefully on each sample. Temporal studies demonstrated that cell adhesion strength and spreading area reached steady-state by 4 hr. Adhesion and spreading studies along with migration experiments demonstrated that NDGA treatment affects cellular behavior on films, partially reducing adhesion strength, migration, and spreading area. However, on the cross-linked gels which are less dense, the only change in cell behavior observed was in migration speed.

We hypothesize that these differences are due to the collapsing of the collagen films. This compaction suggests a less open organization and could be allowing the collagen fibers to form more inter-chain bonds as well as bonds with the small NDGA cross-linker; while NDGA treatment of the fully hydrated gels may rely more on NDGA polymerization to span the greater distance between collagen fibrils. From these results, we can determine that the chemical/physical masking of the adhesion sites by NDGA on collagen films affects cellular behavior more than the masking that occurs in the cross-

linked gels. Although this study shows an effect in cell behavior on the cross-linked films, it also demonstrates that cells can adhere and migrate to this NDGA biomaterial supporting the idea that this biomaterial can be utilized for tendon replacement.

CHAPTER 1: INTRODUCTION

1.1 Tendons

Tendons are essential tissues that connect muscles to bones. The extracellular matrix (ECM) is made up mostly of Type I collagen (about 30% of the total weight) and elastin (2%), a protein that permits the tendons to be flexible. The rest of the tendon is primarily composed of water and tenocytes (cells that reside in the tendon) [1, 2]. Tendons are characterized as being stiff and flexible; they are able to stretch approximately 4% without becoming damaged [3].

The primary function of the tendon is to transmit forces from the muscles to the bones, permitting movement of different sections of the body by the motion of the joints. These connective tissues are stronger than muscles and capable of supporting weights that are 17 times heavier than the regular body weight. The strength of the tendon depends on the properties of the collagen fibers such as their size, thickness, orientation, and fibrillar organization. The quantity of tendon fibers utilized in a certain movement is also important to the overall tendon force. [4]

When a load is applied to the collagen fibers, the fibers rearrange themselves immediately parallel to the direction of the load. However, not all tendons are oriented in a parallel pattern; some are arranged longitudinally or in other forms, depending on the location and specific function of the tendon. Tendons also vary in shape and size depending on their location. [2]

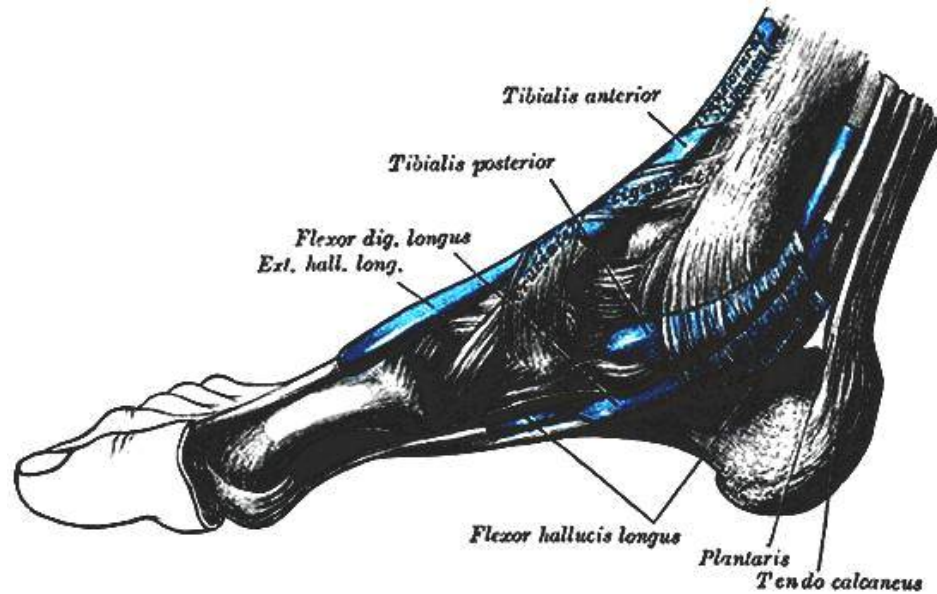


Figure 1 The Achilles tendon (Gray, 1918 - public domain). [5]

There are various types of tendons; however, the strongest tendon in the body is the Achilles tendon (shown above). The Achilles tendon connects the calf muscle to the heel bone, it allows a person to walk, run, and do other activities. Although fibrous sheaths protect tendons when they are being stretched by the bone-muscle movement; sometimes they cannot prevent them from becoming ruptured or damaged. [2]

Damage to the tendon is most likely to occur in athletes that work their muscles more extremely than the normal population. Other factors that reduce the tendon's properties, which ultimately affect and damage the tendon, are aging and the use of steroids [2]. Although all tendons are very important for proper body functionality; tendons located in the hand are the most difficult type of tendon to repair due to the higher likelihood of peripheral adhesion and scar formation post surgery. For this reason, a focus on flexor tendon repair through the development of a slowly degradable replacement will be taken.

1.2 Tendon Healing Process

The three stages of the healing process are the inflammatory phase, the fibroblastic phase also known as the collagen producing phase, and the remodeling phase. The inflammation stage usually lasts approximately 2 to 3 days following surgery; during this stage inflammation occurs after the repair of the tendon. Inflammation often occurs either due to the suture utilized in the surgery or due to fibrin clots that may be located at the ends of the tendon. Once this stage is complete the healing process continues with the fibroblastic phase which lasts roughly 5 days to 4 weeks. [6]

During the fibroblastic stage, fibroblasts migrate to the injured site, proliferate, and secrete new extracellular matrix. Peripheral adhesion occurs when tendon healing it is dominated by extrinsic factors; as the tendon is covered by the sheath, the extrinsic fibroblasts residing on the surrounding tissues of the tendon arrive to the injured site and begin to proliferate, overwhelming the tenocytes remaining in the injured tendon site. On the other hand, a reduction in peripheral adhesion occurs if the fibroblasts residing within the tendon populate the injured site and produce the new extracellular matrix. Therefore, the rapid rise of tensile strength throughout this stage could be due to the scar formation and production of extracellular matrix. [6, 7]

The fibroblastic period is followed by the remodeling phase which can last for months. During the course of this stage, the newly formed tissue becomes reorganized into a network of collagen fibrils that begin to align parallel to the direction of the load. Once this stage is complete the tendon will re-gain some of its strength and functionality; however, it will never fully recover its properties and become fully functional. [6, 7]

The limited number of fibroblasts that reside in adult tendons are very dispersed within the fibrous phase; for this reason, they were first considered to be unable to proliferate and produce extracellular matrix. Nevertheless, after several studies it was discovered that these resident fibroblasts produce and organize collagen and other macromolecules into a fibrous phase parallel to the direction of the tensile load. [7]

Scientists have performed *in vivo* and *in vitro* studies to show that cells that reside on tendons respond to mechanical changes. Banes [8] and Hannafin [9] performed *in vitro* studies with cells isolated from tendons to show that fibroblasts respond to mechanical loads. Furthermore, Malaviya [10] and Woo [11], demonstrated that cells produce biochemical alterations when they are exposed to different mechanical stresses.

Banes et al. [8, 12, 13] also demonstrated that fibroblasts that reside in the tendon tend to respond to induced strains via stretch activated channels. Prior to Banes discovery, McNeilly et al. had indicated that tendon fibroblasts respond in a coordinated manner due to their interconnection through cellular processes as well as gap junctions [14]. After these findings, it was determined that the proper biomaterial for tendon replacement should enable a direct attachment of cells (fibroblasts) that will endure the appropriate strains when loaded [7].

1.3 Tendon Healing Techniques

Due to their continuous usage, tendons tend to become damaged when they suffer either one of two types of ruinous failures: accidental lacerations or extreme instantaneous loads. Tendons contain collagen fibers and fascicles that are organized in a linear manner along the longitudinal axes. [7] Their hierarchical organization provides

the necessary strength for the tendon to handle its specific job in the body. However, this complex organization also makes it difficult for doctors/scientists to repair tendons and create techniques that will recover most of the tendon's original strength and movement.

Although there is a tremendous amount of research on methods to repair different types of damaged tendons, an enormous quantity of this research has focused on the repair of digital flexor tendons since there are more complications during surgery due to the higher likelihood of peripheral adhesion and scar formation. Therefore, the following suturing section will mostly focus on flexor tendon repair.

1.3.1 Suturing Techniques

Doctors who practiced medicine prior to the 1960s believed in the concept of “no man's land” when faced with patients who had digital flexor atrophies. This theory stated that no repair should be done on tendons divided in the digit; however, this was later proven to be inaccurate. [6] Most of the suturing techniques nowadays utilized either core or circumferential sutures to repair flexor tendons. A group of scientists including Komanduri [15], Savage [16], and Silfverskiold [17] determined that the strength of the repair is dependent on the number of times the suture strand is crossed over the site of repair. It was also determined that post-surgery problems were often due to a rupture of a suture knot. [6]

Other researchers such as Pruitt et al. [18] showed that gapping is the weakest part of the tendon. Gapping does not only draw tendon adhesion in the repair site but also damages the mechanics of the tendon. From the above studies and his own studies, Dr. Strickland [19] concluded that a principal flexor tendon repair should have minimal gapping at the repair site, minimal interference with the vascularity surrounding the

tendon, secure suture knots, and sufficient strength to allow early tendon movement. The tensile strength, the properties of the sutured tendon-gap units, and the efficiency of the gliding of the repair site must also be considered when designing a suturing technique. [7]

Although various suturing techniques have been established to join and reduce any gaps found in the tendon. These current suturing techniques do not offer the necessary mechanical strength to handle the same loads handled by a normal tendon [7]. Therefore, other techniques and materials are being developed in an attempt to solve this problem by enabling easier suturing.

1.4 Materials for Tendon Healing

Researchers continue to investigate and create different materials that have the potential to be utilized for tendon repair. These materials range from tissue grafts extracted from another source (human or animal), to a variety of biomaterials. Only certain materials will be noted in this section in view of the fact that an immense amount of materials are being investigated in this field.

1.4.1 Tissue Grafts

Tissue grafts are often used in surgeries to replace certain damaged tissues in the body. They are categorized as autografts, allografts, or xenografts. The easiest and most reliable graft is the autograft which is taken from a specific individual and then implanted back into the injured site in the same individual. These grafts are frequently studied because of their ability to keep the necessary biochemical properties of the extracellular matrix. They also reduce immune reactions and other rejections that may be caused after

implantation. Common examples of autografts are tendons utilized for anterior cruciate ligament repair. [7, 20]

Even though autografts have more advantages than other types of grafts, the technique to obtain this graft is very limited and time consuming since only a certain amount of tissue can be taken carefully from a person without compromising the graft during the resection. [20]

Allografts, on the other hand, provide a greater source of structural material needed during tissue repair. These grafts are taken from human corpses and as a result the cleaning process is more rigorous. To reduce immunogenic responses these tissues must be treated and cleaned by removing all the blood, cells, and other proteins that are found within the tissues. Unfortunately, even if these grafts are cleaned properly and able to retain their biochemical properties, inflammatory responses still occur. [20]

The last and most problematic way to obtain tissue grafts is by removing tissues from animals, i.e. bovine or porcine sources. Although more grafts can be obtained using this method, it takes more effort, time, and money to remove all the unnecessary materials found in those tissues making the FDA approval process even more complicated than the one for allografts. [21]

1.4.2 Synthetic Materials

Scientists have also explored various synthetic materials that could be use for tendon repair; some of these materials include carbon fibers, nylon, silicone, and Teflon [7]. Mendes et al. developed a carbon fiber strand comprised of long cylindrical collagenous fibers with cells that surround the center of each carbon fiber. Dogs' tendons were replaced with these carbon fiber strands for histological investigation. The study

demonstrated that the irritation of the tissues, caused by the carbon fibers, reduced the density of collagen within the tissue affecting the healing repair. [22]

Other researchers utilize more than one synthetic material in an effort to construct an ideal implant for tendon repair. Hunter et al. performed a study of an implant that consists of a silicone rubber with a Dacron center that terminates in a loop at the proximal end and a metal plate at the distal end. From the experimental analysis, it was concluded that this material could be useful in tendon implantation surgeries. [23]

Many studies like the one done by Hunter et al. strengthen the idea that synthetic materials could be use as tendon repair implants. Nevertheless, the only synthetic material that has been presumed to be useful in the fixation of torn rotator cuffs and Achilles tendon' ruptures is the Leeds-Keio ligament. [7]

The Leeds-Keio ligament is assembled with polyester fiber, shaped in the form of an open-weave mesh and containing rectangular holes. This implant has been studied in various parts of the body. Fujikawa et al. demonstrated that of several patients who had patellar ligament or quadriceps tendon surgery with this material implantation found that immobilization was not necessary post surgery. Also, unlike other synthetic materials, no cases of infection were found in this study. [24]

Apart from the Leeds-Keio ligament, other implants constructed with synthetic materials often induce some kind of body response which can either be an inflammatory response, an antigenic reaction, or both [7]. During these responses, the body immediately sends cells to the affected area to attempt to destroy the implant; this ends up not only affecting the tendon' repair, but also causing additional damages to the body. Therefore, even though synthetic materials can handle strengths similar to that of the

human tendon, problems with biocompatibility demolish any possibility of them being utilized in any current clinical applications.

1.4.3 Other Biomaterials

Tissue engineering is a fast growing field, with the purpose of improving the quality of human life by discovering biomaterials that can repair tissue malfunctions inside the body (i.e. tendon injuries). This repair can be accomplished by manipulating cellular and biochemical factors that influence tissue remodeling. [25]

Most cells in the body need to be in contact with a surface in order to survive and proliferate adequately. Therefore, surface's properties are important factors that must be considered when designing a biomaterial. Some of the surface properties that are often taken into account when developing a useful biomaterial are hydrophobicity and roughness. [26] Cell-surface interactions are also essential when designing a biomaterial and for this reason throughout the years scientists have completed several studies on how to control cell function by engineering biomaterials [27].

Various research groups are searching for the best methods to differentiate cells into distinct tissues by designing biomaterials with properties that direct cell function and which can be implanted. Usually these tissues are developed by combining cells and growth factors within a natural or synthetic scaffold. Stem cells are often utilized because of their ability to differentiate into various tissues when combined with progenitor cells or appropriate signals. [7]

Many biomaterials known as natural biomaterials are created with components found inside the body to reduce the possibility of implant rejection. The materials' design is based on the tissue that needs to be repaired; mechanical and chemical properties tend

to vary accordingly to these tissues. For example, cells in the brain are located in a soft environment with stiffness of approximately 2500 Pa, while cells that reside in the bone are accustomed to stiffer materials. [27]

Tissues in the body become stiffer when problems such as diseases produce scar formation and tumors. Jacot et al. found that substrates with a stiffness of 1kPa have similar properties to soft tissue, while the substrates with a stiffness of 50kPa have similar properties to myocardial infarction-like tissue [28]. Whereas, Paszek et al. [29] demonstrated that tumors are significantly stiffer than regular tissue; breast cancer tumors have a stiffness of roughly 4000 Pa while the stiffness of normal tissue is about 150 Pa.

Several investigations have been made to understand how cells behave in their normal environment as well as in the scar tissue/tumor environment. The knowledge gained from these studies helps scientists find the best technique to repair distinct tissues. For instance, Awad et al found that there was a significant increase in modulus, stress, and strain energy density in defected patellar tendons that were treated with a tissue-engineering implant that consisted of collagen gels containing mesenchymal stem cells (MSCs) [30]. Young et al. also demonstrated an improvement in biomechanics repair after MSCs entrapped in collagen gels had been delivered to rabbit Achilles tendons. [31]

1.5 Collagen

Collagen is the most abundant protein found in the body, approximately 90% of the dry weight of tendon is composed of collagen [7]. Tropocollagen, the structural unit of collagen, is approximately 1.5 nm in width and 280 nm in length. The tropocollagen molecules are composed of three alpha chains, with different amino acid sequences, that

form a helical shape as they are wrapped around each other. As each amino acid sequence varies, it forms a different type of collagen. [2, 32]

There are 1000 amino acid residues in each alpha chain; however, glycine, proline, hydroxyproline, and hydroxylysine are the four major amino acids found in these chains. Glycine, the most common amino acid, makes up approximately 33% of the entire collagen and it is found in every third amino acid within the sequence. [2, 32]

Each of these amino acids is believed to play an important role in the formation of fibrils as well as in the increase of collagen's strength. The job of hydroxyproline is to connect the three alpha chains (also known as procollagen molecules) together by hydrogen bonding, while the small glycine residues allow the alpha chains to join together very closely forming a procollagen molecule. Once these procollagen molecules are formed they again bind to each other in a helical manner, thanks to the hydroxylysine amino acid which covalently cross-links these tropocollagen molecules into bundles. The tropocollagen molecules self assemble with a head to tail interaction. [2, 32]

These newly formed fibrils are 67 nm wide and based on the arrangement of their amino acid sequences they form different types of collagen. Gap regions found within the fibril are formed when there are spaces between the heads and tails of tropocollagen molecules located in different rows. Due to these gaps, collagen displays dark and light band under electron microscopy; the dark bands representing the gap regions. [32]

The natural cross-linking of the collagen fibril leads to the formation of the main unit of the fiber system which is found in all connective tissues. Once these mature fibrils align, they begin to bundle with each other producing fibers. These fibers once again align to each other and bundle to form fascicles or bundle fibers which are found in

tissues such as tendons, shown in Figure 2. The collagen fibril organization allows for the formation of tissue's structures which are necessary for the proper function of the tissues.

[20, 32]

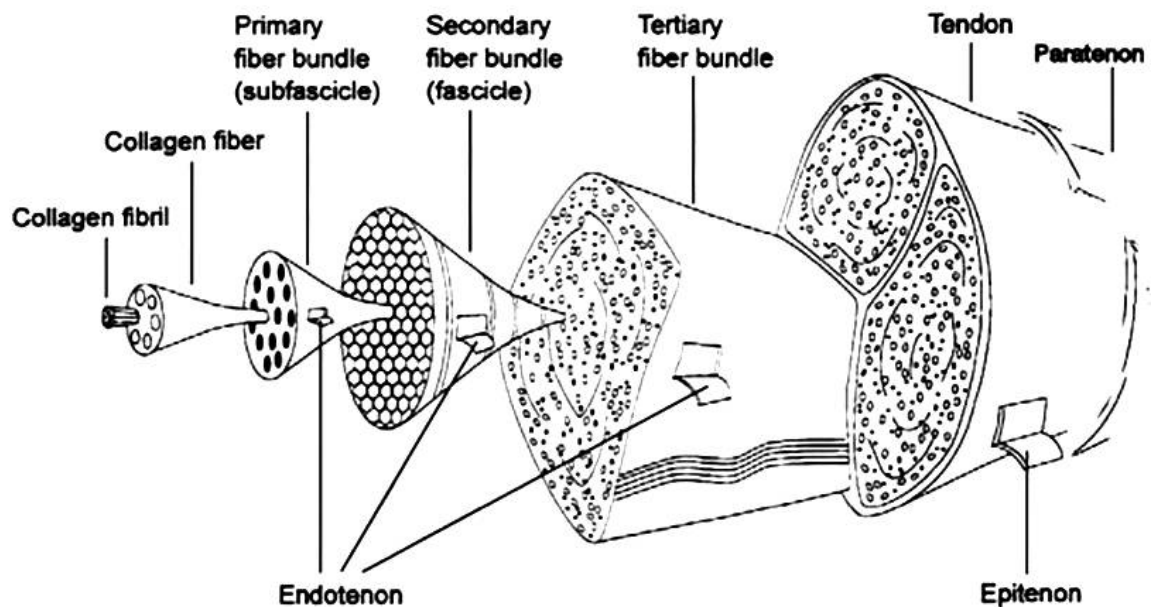


Figure 2 Collagen fiber formation. Picture taken from Fedorczyk 2012. [33]

The alignment of the fibrils and fiber bundles is based on the type of cell that is synthesizing the collagen. The specific cell type is responsible for orienting the fibers and pulling them around to fit them to the required shape, which depends on the tissue being formed. [32]

1.5.1 Collagen Type I

Scientists have discovered more than 20 types of collagens that differ based on the combination of alpha chain sequences [21]. Each type of collagen is organized and assembled with other types of collagen depending on their tissue location [20]. In this

study, we will focus on collagen type I since it is the major component of tendon dry mass and it is the most abundant collagen found in the body [20, 21].

The major function of collagen type I is to resist tension. This collagen is composed of two alpha 1 chains and one alpha 2 chain. Collagen type I is found in various parts of the body, including the dermis, ligaments, bones, organ' capsules, and tendons; for this reason, fibroblasts, osteoblasts, odontoblast, and cementoblasts synthesize this collagen in their respective tissues. [21]

1.5.2 Utilization of Collagen in Biomedical Applications

Collagen is commonly used as a biomaterial because of all its properties, especially its native structure. The assembly of its fibers provides the necessary support to the structures of all the tissues found in the body and also gives it the ability to arrange itself into scaffolds to achieve the required physiochemical properties necessary for a specific implant. [20] Collagen is utilized for biomedical applications in different forms such as collagen fibers and reconstructive fibrils.

1.5.2.1 Collagen Fibers

The use of collagen fibers for the production of scaffolds is a strategy that takes advantage of the structure of collagen. Collagen fibers are often employed for prostheses manufacturing, they can be treated as an allograft as long as the fibers are handled properly. Proper handling ensures that the biomechanical properties of collagen are being retained which leads to proper functional properties of the tissues. Once clean, these naturally cross-linked collagen fibers, commonly known as insoluble collagen, are reassembled and fixed during prostheses' production. [20]

Collagen fibers are produced from tissues found in the body, such as the Achilles tendon. Nowadays the tissues being employed for the production of insoluble collagen are taken from animals. Although the reassembling process of these fibers is complicated, it provides scientists the opportunity to shape fibers in different structures and with various geometries/sizes that satisfy the necessary graft production requirements. So far some of the biomaterials composed of insoluble collagen fibers have been developed for tendon and ligament repair. [20]

1.5.2.2 Reconstructive Fibrils

Reconstituted fibrils from native collagen are also utilized for various biomedical applications such as collagen scaffolds' production. These fibrils are obtained from tissues that contain collagen molecules that have a sequence of amino acids also known as telopeptides. There are two techniques that can be employed to obtain reconstituted fibrils: acid extraction and the digestive enzyme method. [20]

The acid extraction technique is done on newborn or growing animals, since telopeptides become scarce once the animal is completely grown. The extraction must occur at a stage where it is easy to alter the acid component; for that reason, this process is completed before the formation of intermolecular covalent cross-links and the advancement of the allysine pathway. [20, 34, 35] Unfortunately, only a small amount of collagen can be absorbed when using this technique.

The enzyme extraction method, on the other hand, allows scientists to acquire a larger amount of collagen. This method employs a digestive enzyme, pepsin, which is treated in acid to cleave the telopeptide region of the collagen that is located in the cross-

linking section. Once this is done, the molecule is absorbed and it goes through purification. [7, 20]

Once the collagen has been extracted, either by the acid extraction or digestive enzyme method, it goes through the purification process. This process utilizes acetic acid and is done with salt fractionation. The collagen concentration is adjusted to 0.7M NaCl by the addition of NaCl in acetic acid. The collagen solution is centrifuged in order to collect the major fibrillar collagen and then re-dissolved in acetic acid. Any remaining salts are removed from the final solution during dialysis. Verification of the purification of the collagen solution is done by an amino acid analysis and electrophoresis. Once the collagen solution is pure, it can be utilized for implant studies since these techniques follow FDA regulation. [20]

It must be noted that the acid extraction and purification protocols mentioned above are employed by the company, MiMedx Inc., that provided the collagen for all the experiments described in Chapter 2.

1.6 Collagen Fixation Methods

Due to its biological properties, collagen is employed in various research laboratories. One of the major focuses of collagen research is in discovering and gaining a better understanding of the different methods available to cross-link collagen. If a collagen material was implanted in the body with no cross-linking reagents, then it will degrade at a fast rate.

The purpose of an implant is to stay in the body long enough to regenerate the damaged tissue; therefore, the collagen material must be engineered in a way to reduce its

degradation rate. It has been found that by using a collagen fixation method, the collagen material will not only have greater mechanical properties, but also stay in the body for the extended periods of time necessary for tissue regeneration.

The viscosity of the collagen solution allows researchers to cast collagen gels on different surfaces and in different shapes. Unfortunately, these gels are very delicate and difficult to handle. Therefore, collagen fixation is also necessary to facilitate the handling of collagen materials for tendon and ligament repairs. [20]

The fixation of collagen is either accomplished as a traditional, physiochemical, chemical, or polymerization approach. Although all these methods are important, this section will focus on the three best studied collagen cross-linkers: glutaraldehyde, carbodiimide, and nor-dihydroguaiaretic acid (NDGA).

1.6.1 Glutaraldehyde Treatment

Glutaraldehyde is the most common reagent employed to cross-link collagen fibers [36]. This very inexpensive aqueous solution is able to cross-link collagen during short periods of time. The glutaraldehyde treatment makes the collagen material stiffer and provides better stabilization than other cross-linking reagents, including carbodiimide, epoxy, and genipin. [37]

This fixation technique covalently cross-links glutaraldehyde with the collagen molecule through the amine groups ($R-NH_2$), as shown in the figure below. The number of bonds that are formed by this cross-linking method is based on the distance between each molecule and the quantity of available amine groups. Even though glutaraldehyde reacts with amine groups, it can also react to a lesser degree with carboxyl groups [20]

The effect of glutaraldehyde collagen fixation varies with the concentration of glutaraldehyde employed to cross-link the collagen material. Unfortunately, as the glutaraldehyde residues start leaving the material, they automatically become toxic to the body. Careful consideration of glutaraldehyde concentration is needed to continue exploring collagen cross-linking with glutaraldehyde for tissue implantations. [37]

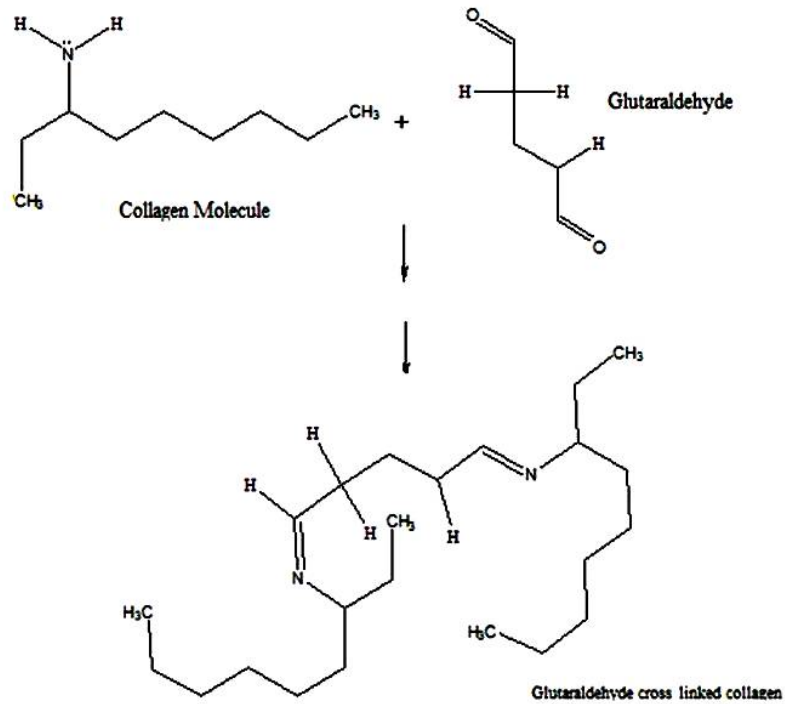


Figure 3 Glutaraldehyde cross-linked collagen.

1.6.2 Carbodiimide Treatment

Unlike the glutaraldehyde method, the carbodiimide cross-linking method does not cause any toxicity problems since all the un-reacted groups can be removed if the proper reagent utilized to activate the carboxylic acid is utilized [38].

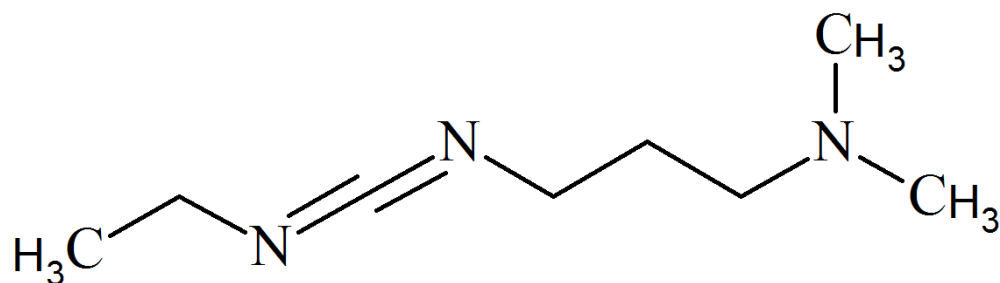


Figure 4 Chemical structure of 1-ethyl-3-(3-dimethylaminopropyl)carbodiimide (EDC).

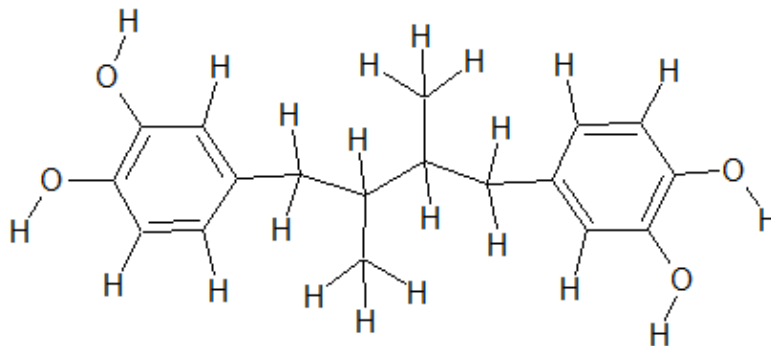
The carbodiimide compound that is most often used for collagen cross-linking is the 1-ethyl-3-(3-dimethylaminopropyl)carbodiimide (EDC) shown in Figure 4. The reaction of this compound with the collagen side chains that contain aspartic and glutamic acid' carboxylic groups, form another compound that reacts with the amine groups of the lysine side chains of collagen generating an amide cross-link [20].

Although this cross-linking method produces a collagen product that is more biocompatible than glutaraldehyde, other cross-linking agents including glutaraldehyde increase the stabilization and tensile properties of collagen more significantly which is necessary for tendon implants. [36]

1.6.3 NDGA Treatment

Nor-dihydroguaiaretic acid (NDGA) is an antioxidant that has a 6-carbon alkane chains with a functional ortho-catechol on each side. The reactive end catechol groups of this antioxidant extracted from *Larrea divaricata* or creosote bush (~ 5 to 10% of the leaves dry weight is made of NDGA), cause polymerization [39]. This polymerization first occurs when these catechols begin to auto-oxidized and become ortho-quinones, at a slow rate and neutral pH [40, 41]; these two quinones proceed to form bisquinones cross-links at the end of the NDGA molecule by oxidative coupling and aryloxy free radical

formation. The bisquinones cross-links are continued, forming a polymer network that ends up entrapping the collagen fibers within it. [39]



NDGA Molecule

Figure 5 Diagram of NDGA molecule.

Although this NDGA mechanism is based on the polymerization technique, recent studies by MiMedx Inc. (Personalized communication with Dr. Thomas J. Koob) have found that NDGA may also be employing the cross-linking technique, bonding itself with the amino acid side chains of the collagen molecule.

This antioxidant treatment provides many benefits to collagen including stabilization, anti-inflammatory capabilities, and enhancement of its mechanical properties. For this reason, it is employed in various medical applications for the treatment of several diseases [39]. Moussy et al. [42] utilized NDGA collagen fibers to develop a local drug delivery system, while Lu et al. [43] demonstrated that by cross-linking NDGA decellularized heart valve scaffold, the biomaterial became more stable, durable, and stronger. In addition to the cardiovascular and drug delivery fields, this biomaterial is also being investigated in the neurological and cancer treatment areas.

Studies done by others have demonstrated that the treatment of collagen fibrils with NDGA can be ideal for tendon tissue replacement. This is because NDGA enhances the tensile properties of the collagen fibrils, making it comparable to the ones of the human tendon and because is not cytotoxic, permitting the cells to attach, migrate, and proliferate within the material. [40]

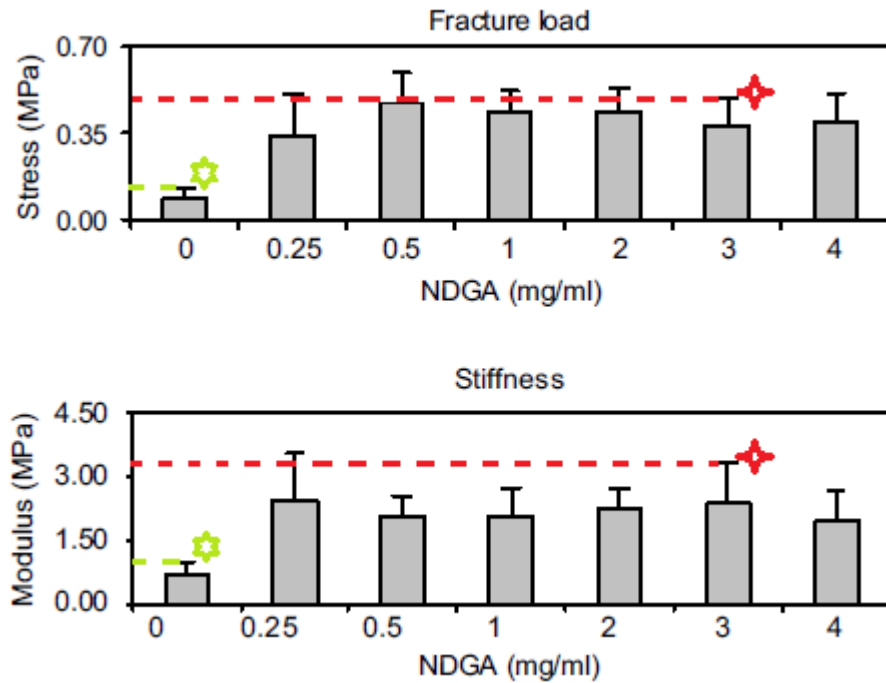


Figure 6 Properties of 5% gelatin gels with different NDGA concentrations. [40]

The figure above taken from Koob et al. [40] shows that there is an increase in stiffness and stress between untreated 5% gelatin gels and the ones treated with 3.0 mg NDGA. The two symbols were added to the figure to show our comparison between the two groups. Although the focus of this thesis is on collagen gels instead of gelatin, we undertake that the relation between the untreated and treated collagen gels will be similar to the ones shown above. This assumption is made not only because gelatin is the product

of denatured collagen but also because previous studies have shown that collagen fibers treated with this concentration of NDGA enhances the tensile properties of the material.

1.7 Adhesion Assays

Molecular interactions occur when ligands and receptors match each other and form conformations. When a good conformation occurs between the cells' receptor and the ligand, the cell adheres strongly to the surface with strong bonds that last for long periods of time. These non-covalent bonds (i.e. hydrogen bonds) are individually weak; however, once they get close together they form strong bonds between the cell and its surface. [44]

Mechanical forces applied to these bonds usually lead to deformation of the receptor, altering the matching conformation between itself and the ligand. The deformation of the receptor can also affect its specificity for the ligand, causing a possible conformational match between this same receptor but to a different type of ligand. All these changes alter the adhesion strength of the cell to its surface. [44]

When cells are seeded on a surface, they originally bind to this surface weakly with a small number of receptors; however, as time progresses they begin to spread on the substrate increasing the number of receptors at the cell-substrate interface. The local increase in number of receptors leads to an increase in bond formation and subsequent enhancement of adhesion force between the cell and its substrate. [45]

The primary family of cell-surface receptors that bind extracellular matrix proteins are the integrins. Integrins are transmembrane glycoproteins composed of alpha and beta chains that link the cell's actin cytoskeleton to the ECM with the aid of other

intermediate proteins [45]. These integrins play a major role in cell adhesion and migration since they facilitate the adhesion of cells to different substrates. [46]

Shear stress, which is a force applied over a finite area, is the measurement utilized to quantify cell adhesion strength [45]. All the techniques utilized for cell adhesion measurements are classified based on the forces employ to detach the cells from the surface. Each cell adhesion characterization technique is considered to be either part of the centrifugation, micromanipulation, or hydrodynamic shear methods. Although all of the techniques are useful, only some of them provide a quantitative measurement of cell adhesion strength. [45, 47]

1.7.1 Centrifugation

The centrifugation method applies centrifugal forces, forces normal to cell adhesive area, which occur when samples are placed in a usual centrifuge. Once the sample has gone through the centrifugal method, the quantity of cells remaining in the surface is compared to the initial number in order to determine the adhesion strength. Various scientists such as Chu et al [48], Reyes et al [49], and Giacomello et al [50] have utilized this method to investigate the strength of the cells on different surfaces. Although this method is very convenient due to its simplicity, it is limited to short term studies and it only allows one single force to be applied at a time. [45]

1.7.2 Micromanipulation

Micromanipulation is the second method that is employed for cell adhesion measurements. Micropipettes, microprobes, AFM cantilever, or laser tweezers are employed in this technique. Various scientists such as McKeever et al. [51] utilized the

micromanipulation technique for studies such as the investigation of the adhesion of alveolar macrophages. Unfortunately, this technique utilizes expensive specialized equipment and it is limited to single cell or receptor-ligand pair measurements. [45]

1.7.3 Hydrodynamic Shear Assay

The third method is the hydrodynamic shear assay which allows for adhesion studies on a larger cell population. This method consists of different flow systems that utilize a variety of forces to detach cells from different surfaces. This technique is considered the most reliable for cell adhesion measurements because researchers have the ability to control and reproduce the forces for different sets of experiments. [45]

Parallel plates, radial flow between parallel disks, and rotating disks are the three systems considered part of the hydrodynamic shear assay classification. They are distinguished from each other based on flow configuration which depends on their geometry.

1.7.3.1 Parallel Plates

The parallel plate technique is often utilized because observations of the attachment and detachment processes can be done directly with a microscope [52]. Several experiments must be done to determine the cell adhesion strength since only one force can be applied per experiment. The radial flow between parallel disks also allows direct observation of the attachment and detachment forces. However, cells at the central flow are subject to complex hydrodynamic conditions. [45]

1.7.3.2 Spinning Disk

Unlike other devices such as the parallel plate where turbulent flow may occur, affecting the controlled hydrodynamic forces being applied to the sample, the spinning disk device applies a well-defined range of forces that are strong enough to detach the cells from their surface while keeping the flow in laminar conditions. [53, 54]

The flow patterns that occur in the spinning disk have been approximated based on the flow patterns that occur in an infinite disk that is spinning in an infinite fluid [53, 55]. Shear stress (τ) is applied at the disk's surface by the creation of a velocity gradient that occurs if an assumption that no slip occurs between the surface of the sample and the fluid [53].

Spinning Disk Device

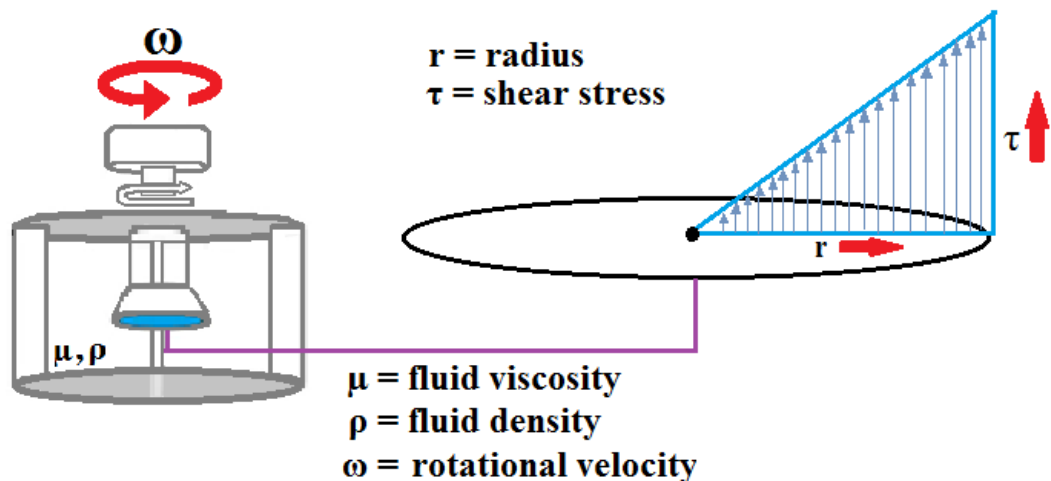


Figure 7 Spinning disk device and radial/shear stress relation (an increase in the radius (r) is related to a linear increase in shear stress (τ)).

As shown by the figure above, a linear relationship exists between the radius and shear stress. Although the radius is an important factor to determine the shear stress, the

fluid density (ρ), fluid viscosity (μ), and rotational velocity (ω) are also necessary to calculate the shear stress applied to a cell at a specific radius. [53]

$$\tau = 0.8r\sqrt{\rho\mu\omega^3} \quad (\text{Eq. 1})$$

Equation 1 demonstrates that at the center of the circle ($r = 0$), cells do not experience any detachment forces ($\tau = 0$). On the other hand, the closer the cells are to the edge, the more detachment forces they must handle in order to remain on the surface. For this reason, the quantity of cells remaining in the surface decreases as the distance of the radius from the center of the surface increases.

After the cells have experienced the range of hydrodynamic shear stress from the spinning disk, sixty-one fields are imaged from the sample and the number of cells remaining in the surface is counted. The fraction of adherent cells left after the spin (f) is then calculated by dividing the cell count of each field by the number of cells located at the center of the circular sample, which experiences zero shear stress. The adhesion profile (Figure 8) is then graphed by plotting the ratio of cells remaining in the surface of the sample versus the shear stress.

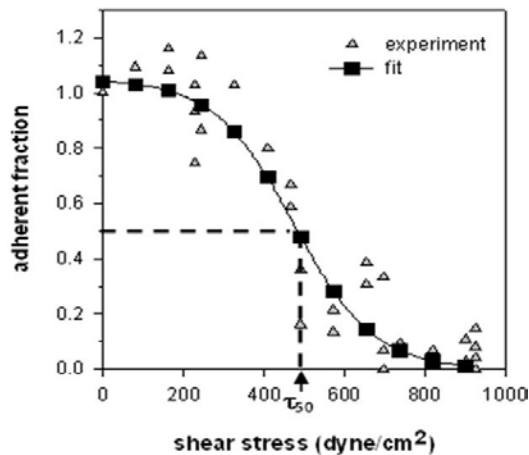


Figure 8 The adhesion profile of a typical cell adhesion curve.

The τ_{50} value from the figure above is calculated after fitting the f vs. τ data to a sigmoid curve (Equation 2) [54, 55]. The shear stress that causes 50% of the cells to detach from the surface (τ_{50}) represents the average adhesion strength of the cells on a specific surface. The adhesion strength will vary based on the location of the sigmoid curve; the adhesion strength increases when the sigmoid curve shifts to the right.

$$f(\tau) = \frac{1}{1 + e^{b(\tau - \tau_{50})}} \quad (\text{Eq. 2})$$

Because of the range of forces and large number of fields analyzed in each experiment, this adhesion strength assay is more robust than other methods and for this reason it is the technique utilized in all the adhesion experiments described in Chapter 2.

1.8 Migration Assays

Cell migration is an important factor in many biological events including wound healing [56], cancer metastasis, and embryonic development. This process involves the mechanical interactions of the cells with the surrounding surface. In order for a cell to migrate, it must go through a process that requires the formation of new attachments from the surrounding ECM as well as detachment from other sites of this ECM. [46, 57]

The migration process is often separated into three different stages. The first stage is when the cell adheres to the environment, the second stage is when the cell generates the necessary forces to propel itself forward, and once this occurs, the cell detaches from the substrate from its rear during this last stage. Integrins not only play an important role in cell adhesion but also are important in cell migration. They augment contractility of the cell and promote changes in the organization of the cytoskeleton [57-60].

Cells first adhere to its surrounding environment by forming membrane protrusions at the leading edge. The existing integrins attach the protrusions of the cells to the ECM and leads them to interact with the actin cytoskeleton. This interaction leads to the formation of focal points, which occurs when various signaling molecules get together at certain sites. The signals then promote contractility in the cells encouraging their propulsion to different sites of the substrate. Once the cells are ready to move to the direction they have propelled to, they begin to detach from the surface at their rear. Although cells leave some integrins on the surface once they detach from the integrin-cytoskeleton connection, they end up taking proteins associated with integrin (i.e. vinculin). The rear sites no longer have integrins forming adhesion complexes making it easier for cell detachment. These same integrins also help in the cell migration process by activating enzymes that can degrade the ECM. [57-60]

There are many variables related to integrin-ligand interactions, such as ligand and integrin levels, which affect the behavior of the cells' migration process (i.e. speed) [61]. It has been predicted by mathematical models [60] that the cell migration speed reaches its maximum when the cell and substrate adhesiveness to intracellular contractile forces, which allow the cell to detach from the rear while forming new attachments at the front, occurs at an intermediate ratio. [61] Rapid cell migration can only occur efficiently when the formation and breakdown of adhesions is continuously going on thanks to the smooth cycling process, from the back to the front of the cell, of various components that are necessary for this migration process. [59]

This migration process is similar for most mammalian cell types; however, this does not mean that all cells migrate at the same rate. Fibroblasts have been found to

migrate 10 to 60 times more slowly than leukocytes due to the fact that they are 3 to 20 times more adhesive to a surface than these other cells. These cells also direct their morphology and migration path based on the coordinated mechanical interactions that occur at hundreds of focal adhesions. [58, 62]

It is also believed that fibroblasts' calcium channels are activated by the stretching that occurs after their contraction at their rear edges occurs. Once activated these channels produce higher calcium levels within the cell which have been found in certain migration studies. [58] Unlike other cells such as keratinocytes which move at a constant velocity in a gliding manner, fibroblasts tend to migrate slower with a reduced extensions and retractions over smaller distances. Higher forces are required to detach fibroblasts from the rear which could be due to their strong attachment to the surface. Scientists have hypothesized that cells that move faster than fibroblasts do not utilize the same amount of integrins employed in the fibroblast migration process. [57]

Various techniques are employed to study cell migration on different surface. The techniques are chosen based on the specific topic being studied, whether it is a two-dimensional or three-dimensional study, or whether the purpose of the study is to understand how fast the cells can repair a wound. Since the focus of this thesis is on fibroblast behavior on 2D collagen gels, the two techniques discussed below are often used for this type of study.

1.8.1 Wound Healing Assay

The wound healing assay is a very common technique employed to investigate cell migration [63]. As the name describes it; this assay works by inflicting a wound to a surface and then observing the behavior of this damaged monolayer during the recovering

and healing process. Prior to forming a wound in the surface, a confluent cell monolayer must be formed. Damage in the surface can be done physically by utilizing an object such as a needle or pipette tip, or electrically by destroying and killing cells with electricity. [64, 65]

Unfortunately, cell migration is not the only factor that occurs in this assay; matrix remodeling, cell proliferation, and cell polarization also take place in the wound healing process. Therefore, it is necessary for the samples to be continuously monitored through the entire experiment in order to differentiate cell migration from other processes occurring within the wound. [64]

1.8.2 Compartmentalization Techniques

The compartmentalization technique is also another method utilized for cell migration studies. Unlike the wound healing assay, no damage has to be done to the surface. A fence or barrier, often in a hollow cylindrical shape, is placed on top of the surface being studied. Cells are seeded inside the cylinder and left inside the incubator the necessary time (usually 24 hr) to allow them to form a confluent monolayer in the circular area. Once this monolayer is formed, the fence is removed from the surface and cells being to migrate outward. [66-68]

Once the targeted migration time has been reached, cells are analyzed to determine the distance they have travelled during this time period. This technique will be utilized in the migration experiments described in Chapter 2 due to its simplicity and its typically reproducible migration results.

1.9 Thesis Objectives

Our major goal is to someday create an optimal tendon prosthetic that can stabilize the damaged muscle-bone connection and then be remodeled by resident cells from the surrounding tissues to ensure long-term function. There are several tendon repair studies that focus on collagen. However, as previously mentioned, scientists have developed NDGA-treated fibers that have tensile properties comparable to that of a human tendon. These fibers have an average tensile strength of 90 MPa and an elastic modulus of 580 MPa [41].

Although studies by Koob et al. [41, 69, 70] have been done on NDGA fibers, our focus was on studying cell behavior on collagen gels/films since they can be formed on cover-slips allowing adhesion measurements to be gathered with the use of the spinning disk. Since it was found that 5% gelatin gels treated with 3.0 mg NDGA were stiffer and stronger than gels treated with other NDGA concentrations, we utilized this 3.0 mg NDGA concentration for polymerization purposes in all our experiments.

Once these collagen samples were manufactured with the same ingredients and protocol utilized to make the NDGA-fibers. Cells were seeded on top of the surfaces and their behavior was studied to determine if NDGA cross-linking affects their spreading, migration, and/or adhesion strength. Based on the results, we will proceed to conclude whether this NDGA-collagen material is adequate for tendon tissue replacement.

CHAPTER 2: MATERIALS AND METHODS

2.1 Cell Culture Reagents

NIH 3T3 Fibroblasts were purchased from the American Type Culture Collection, (Manassas, VA). The culture reagents Dulbecco's modified Eagle's medium (DMEM), 10% newborn calf serum (NCS), and 1% penicillin-streptomycin (P/S) (Invitrogen, Carlsbad, CA) were mixed to produce the complete growth media utilized in all cell experiments. Other reagents employed in the experiments described below, including Dulbecco's phosphate-buffered saline (DPBS), CellTracker Green CMFDA C2925, and Hoechst-33242, were purchased from Invitrogen (Carlsbad, CA).

2.2 Collagen Gel and Film Preparation

Type I R&D bovine collagen (0.5%) in hydrochloric acid (HCl) solution, provided by MiMedx Inc., was utilized to manufacture the gels and films for all the experiments. The details of the purification and preparation of this collagen is described by Koob et al [41]. The acidic collagen solution was stored at 4°C to prevent gel formation, which occurs over time. The final collagen solution was produced by combining the collagen-HCl solution with a salt solution (pH 7.4), composed of 105 mM NaCl and 53 mM NaH₂PO₄ in deionized water, in a 1:1 ratio and adjusting the pH to 7.2. Circular glass cover slips (25mm diameter) were utilized as supporting platforms for the collagen gel formation. The cover slips were cleaned with a compressed nitrogen gun and

then oxygen plasma treated (PE50; Plasma Etch, Carson City, NV) for 5 minutes to remove any residues.

The cover slips were immediately exposed to 0.2% 3-aminopropyl-trimethoxysilane in toluene solution for 30 minutes, and after that rinsed with 70% ethanol. They were subsequently immersed in a 4% glutaraldehyde in ethanol solution for an additional 30 minutes. The silane and glutaraldehyde treatments were necessary for collagen to strongly adhere to the glass surface. Samples were rinsed once again with 70% ethanol, dried with a compressed nitrogen gun and placed inside 35mm tissue culture dishes (TCDs).

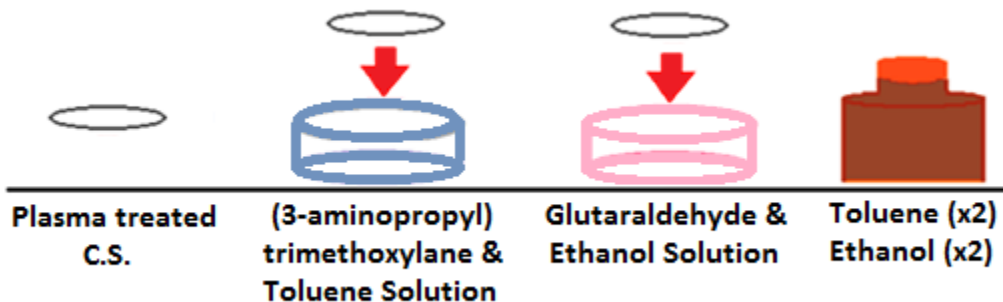


Figure 9 Activation of glass cover slips with amine groups.

200 μ L or 800 μ L of the collagen solution was dispensed on top of the treated cover slips and placed inside the incubator at 37°C, 5% CO₂ for a minimum of 4hr to ensure complete formation of collagen fibrils. The 200 μ L gels were left inside the incubator so they would remain hydrated; whereas the 800 μ L gels were taken out, rinsed with deionized water (DI) water (3mL), and placed on the rocker for 10 minutes (2X) to ensure salts were removed from the gels.



Figure 10 Rinsing of 800 μ L collagen gels with deionized water.

Each gel was carefully wiped to remove any leftover water from the glass and left out to dry overnight at ambient temperature, on top of Parafilm sheets. Once these samples were completely dried, they were considered films instead of gels due to their collapsed structure and reduced thickness.

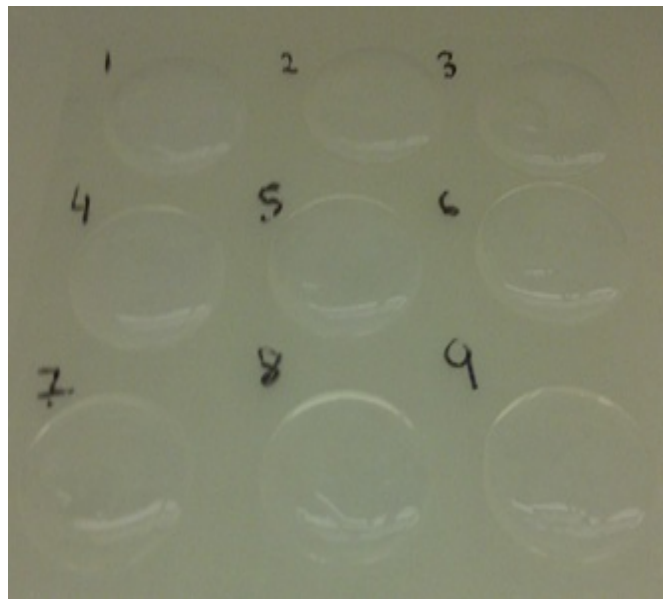


Figure 11 *Wet* collagen gels (800 μ L) left to dry overnight to form films.

It must be noted that the 800 μ L gels which have four times the collagen volume of the 200 μ L gels required a more stringent rinsing to remove most of the salts from their surfaces. Removal of these salts was done to prevent any negative effects of high salt concentrations on cell attachment or survival.

2.3 NDGA Cross-Linking

Once the gels/films were cleaned and manufactured accordingly to their specific treatment shown above, they were exposed to a similar NDGA treatment. The protocol for NDGA treatment was based on the procedure designed by Koob et al [40]; however, modifications were made for the fabrication of *wet*, *dry*, and *re-hydrated* collagen gels/films.

2.3.1 Films - NDGA Treatment

The NDGA powder from Cayman Chemical Company (Ann Arbor, MI), was dissolved (30mg/mL) in 0.1M NaOH. The solution was vortexed to assure the powder was completely dissolved in the NaOH solution. 18mL of 0.1M NaH₂PO₄ (pH 9.0) solution (Fisher Scientific) was then added on top of the NDGA/NaOH solution and mixed thoroughly for a final concentration of 3.0 mg/mL. 2mL of the cross-linking solution was dispensed atop of each collagen film positioned inside a 35mm polystyrene culture dish. The films covered in the cross-linking solution were placed on top of a rocker at the maximum speed for 24hr to allow complete NDGA polymerization in the presence of ambient oxygen.



Figure 12 NDGA cross-linking of 800µL collagen films.

The solution was aspirated, and 2mL of 0.1M NaH_2PO_4 solution was added to each film. This solution was left inside the 35mm tissue culture dishes for 1 hour to assure that any un-reacted residue was completely removed from the cross-linked samples. The films were also washed 3X with DI water (20 minutes each time) to prepare the samples for the cell seeding procedure.

Koob et al. not only demonstrated that good rinsing eliminated un-reacted intermediates from collagen fibers but also that this rinsing made the cross-linking process more effective [41]. For this reason, the films were placed on top of the rocker at the maximum speed during their NaH_2PO_4 solution and DI water rinses. Once the films were completely washed, they were placed on top of Kim Wipes to remove any excess water. After that, they were left to dry overnight on top of a Parafilm sheet to avoid the collagen samples from attaching to the TCDs.

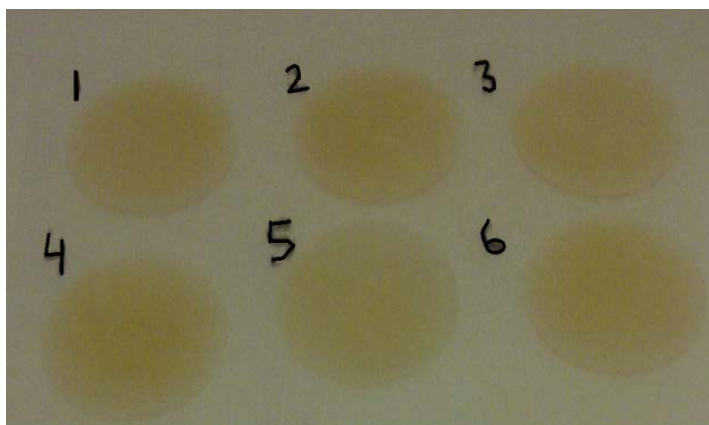


Figure 13 *Dry* NDGA cross-linked collagen films (800 μ L) left to dry overnight.

The figure above shows the 800 μ L *dry* collagen films following their NDGA cross-linking and rinsing treatments. The films are no longer transparent; instead they take the brownish color of the NDGA solution.

2.3.2 Gels - NDGA Treatment

The NDGA treatment of the 200 μ L *wet* collagen gels is very similar to the one employed for the 800 μ L *dry* films. However, instead of leaving the gels to dry overnight, they were placed in new TCDs inside the safety cabinet. The TCDs were then covered with 1mL of 70% ethanol and left for at least 12 hours under UV treatment.

Once all the gels were completely cross-linked, they were rinsed with ethanol for 5 minutes prior to starting seeding experiments to assure that samples were completely sterile and that there was no un-reacted intermediates left that could disrupt cell-surface interactions. Unlike the brownish color taken by the 800 μ L NDGA cross-linked films, the 200 μ L cross-linked gels had more of a yellowish color.

2.4 Absorbance of Collagen Networks

Absorbance measurements of collagen control and NDGA cross-linked samples were completed using the Synergy HT Multi-Mode Microplate Reader (Biotek Instruments, Inc). The optical density (O.D.) was measured over a broad range of wavelengths to determine if the collagen samples were properly cross-linked with the NDGA cross-linking solution.



Figure 14 Synergy HT multi-mode microplate reader (Biotek Instruments, Inc).

These results were compared to the ones completed by MiMedx Inc. in order to determine whether the gels were being cross-linked in the same manner (*see results section*). By doing so, the understanding of the *in-vitro* characterization done in the following experiments will be useful for the NDGA-collagen materials designed by MiMedx Inc.

2.5 Gel and Film Thickness Measurements

2.5.1 Thickness Measurements Using Contact Angle Software

A Contact Angle Measurement (CAM) device (KSV) was utilized to take side-view images of the collagen gels. An image of a millimeter ruler was also taken in order to create a conversion factor of pixels (px) to millimeters (mm): 5 mm = 487.86 px.

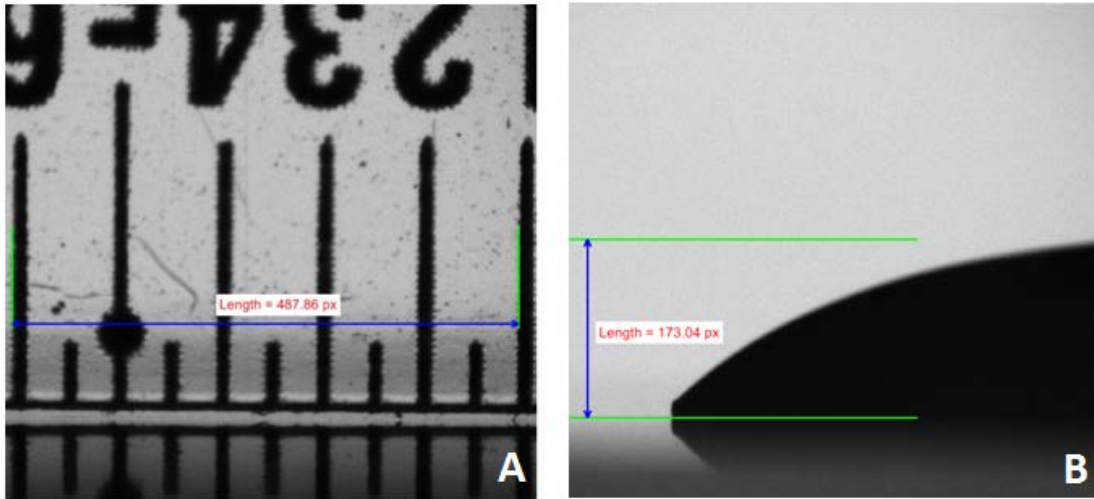


Figure 15 Images taken with contact angle software- Part I. (A) Image of a millimeter ruler. (B) Image of 800µL *wet* collagen gel.

Once the conversion factor was determined, the thickness of each gel was calculated as shown below.

$$\frac{5 \text{ mm}}{487.86 \text{ px}} * 173.04 \text{ px} = 1.77 \mu\text{m}$$

Measurements were done on at least 3 samples to determine the average thickness of the 800µL *wet* collagen gels, as well as of the 200µL *wet* collagen gels, the 800µL *re-hydrated* uncross-linked and cross-linked collagen films. Collagen samples were

weighted before and after the drying process to determine the reduction of collagen volume due to water loss, which was found to be approximately 90%.

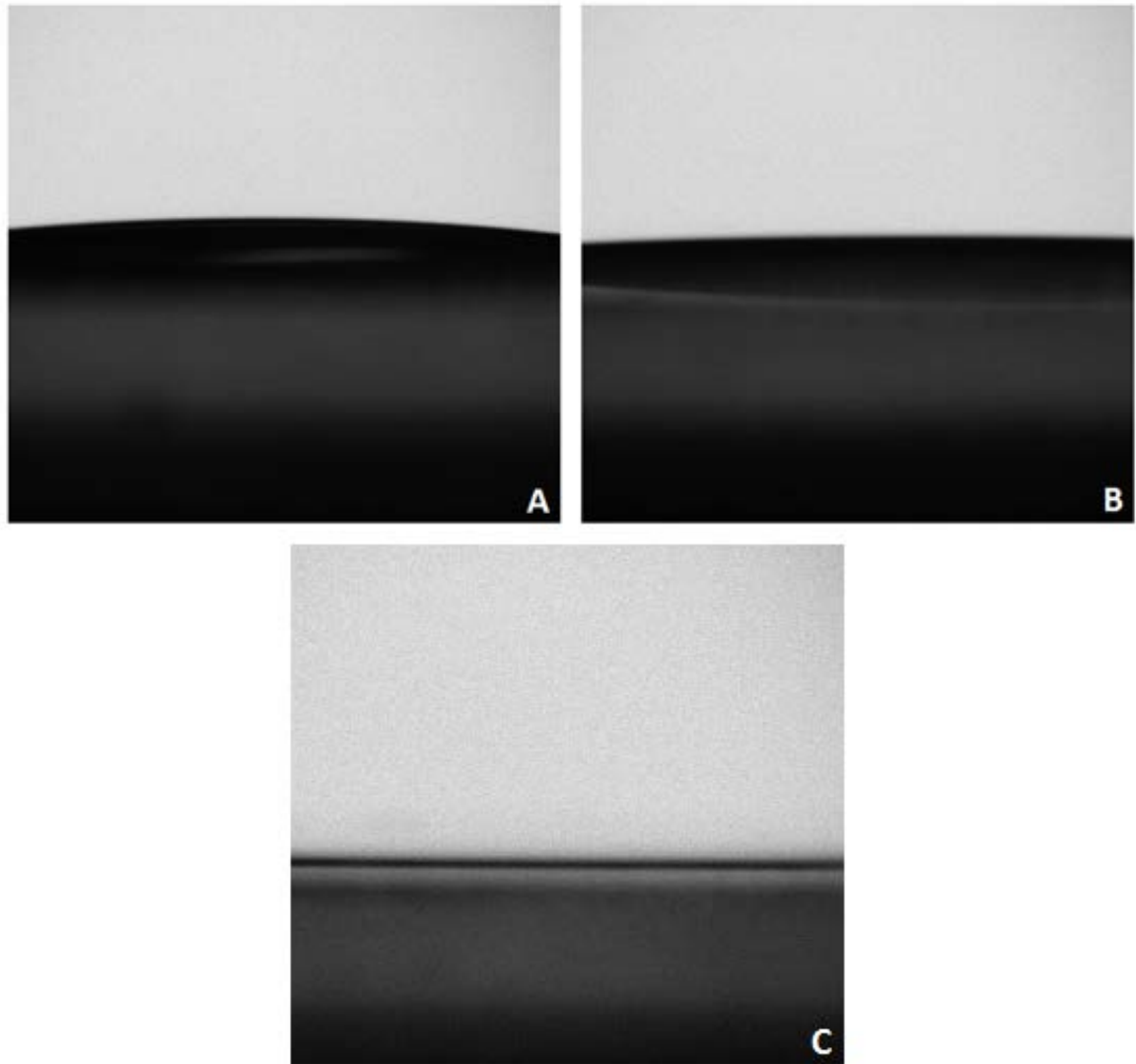


Figure 16 Images taken with contact angle software- Part II. (A) Image of 200 μ L *wet* collagen gel. (B) Image of 800 μ L *re-hydrated* uncross-linked collagen film. (C) Image of 800 μ L *re-hydrated* cross-linked collagen film.

Unfortunately, the thickness of 800 μ L *dry* films could not be calculated using the contact angle software because films are too thin to be differentiated from the glass cover-slip (shown below).



Figure 17 Image of 800 μ L *dry* collagen film using the contact angle software.

2.5.2 Contact Profiler Measurements

The Dektak 150 Surface Profiler (Veeco Instruments, Inc.) from NREC was employed to measure the thickness of the 800 μ L *dry* collagen films. Half of the collagen surface was scratched off the sample in order to measure the thickness of the *dry* collagen samples. The profiler (radius of 12.5 μ m) measures the sample by touching its surface along the horizontal axis.

The results displayed by this software (shown in figure below) are in the form of line profiles of the vertical displacement when the needle goes from the collagen surface down to the glass surface. The two flat horizontal surfaces are selected (the left one being collagen and the right one glass). The distance between the two gives the thickness of the samples; in this technique the thickness is given in Angstroms (\AA) is 48,200 \AA which is approximately 4.8 μ m.

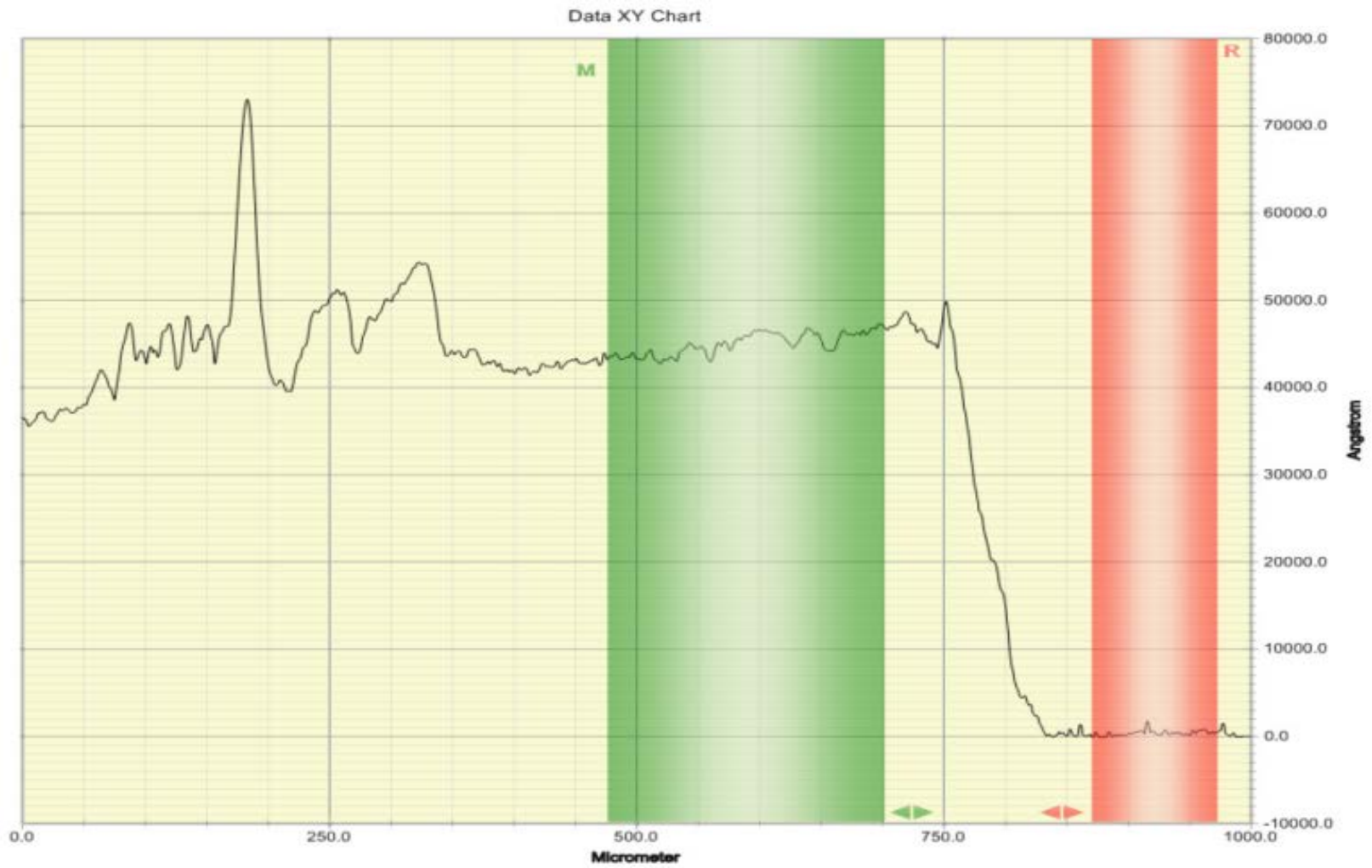


Figure 18 Graph of thickness of 800µL *dry* collagen gel using contact profiler (x-axis: micrometer, y-axis: Angstrom).

2.5.3 Optical Profiler Measurements

To corroborate the thickness of the 800 μ L *dry* collagen films, the Wyko NT9100 Optical Profiler (Veeco Instruments, Inc.), located in the Nanotechnology Research and Education Center (NREC) was utilized. The optical profiler is able to calculate a difference in thickness between two surfaces without physically contacting the samples. The samples analyzed using this equipment were the same samples measured in the contact profiler, which had half of the surface scratched off.

The 3D profiler utilizes white light that does not contact nor destroy the samples being measured [71]. Three dimensional interactive maps (one is shown below) of collagen-glass samples were acquired using this equipment. The glass surface can be seen in blue, which means that the software considers this plane to have a height of zero. The collagen sample, which can be seen on the left side of the figure below, has a green color which represents a height of approximately 5 microns (μ m).

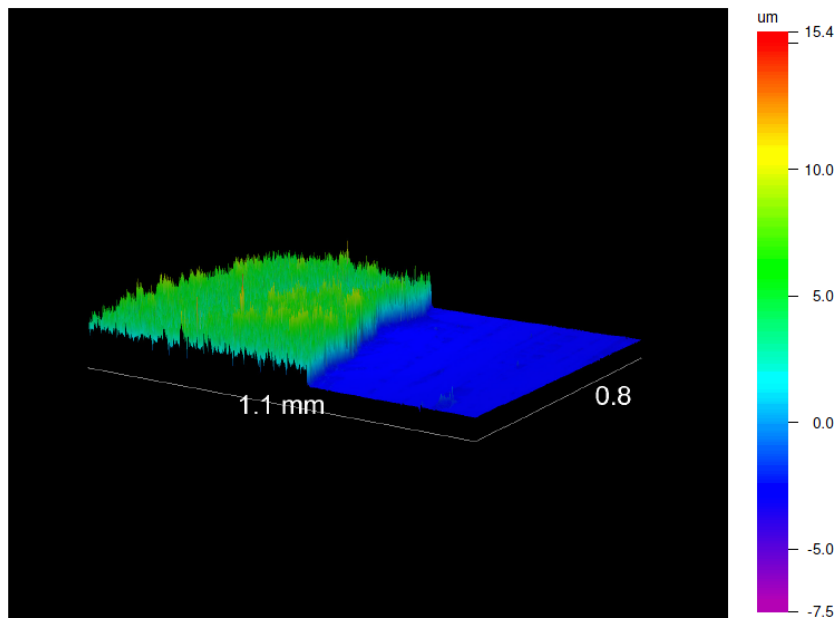


Figure 19 Three dimensional interactive display of collagen - glass border with optical profiler.

To get a numerical value of the thickness of the collagen film, the x-profile analysis (shown below) was utilized. This graph automatically provides a height difference (Z-value) between the two horizontal surfaces. In this case, the height difference is 5.3 μ m which is the average value of the thickness of this collagen film.

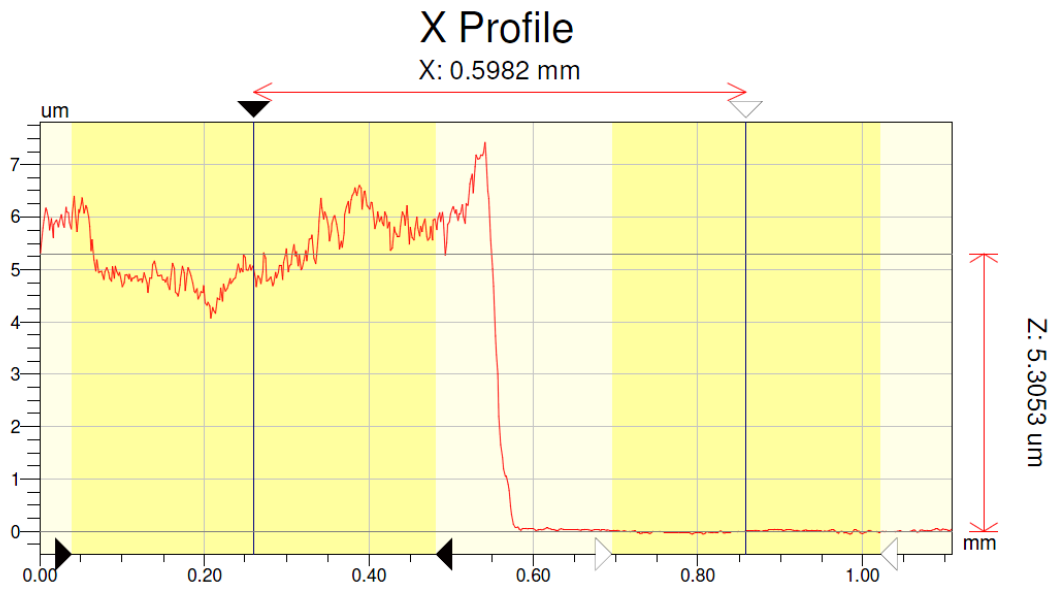


Figure 20 X-profile graph of thickness of 800 μ L *dry* collagen film using optical profiler.

2.6 Cell Adhesion Strength Experiments

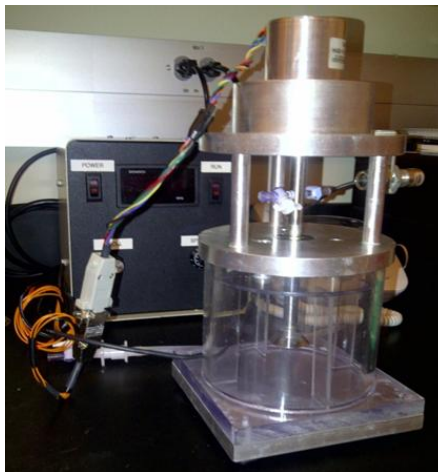


Figure 21 Diagram of spinning disk device.

Hydrodynamic flow systems are among the most reliable methods used to measure adhesion strength since a wide range of detachment forces can be applied to large cell populations. Of these, the spinning disk device (shown in Figure 21) applies a linear range of forces for detachment under constant and uniform conditions at the surface. [45]

The collagen samples containing the cells were taken out of the incubator and placed on top of the spinning disk platform. Application of the vacuum was done to assure that the samples would stay in the platform during the spinning process. The valves were closed immediately to maintain the vacuum seal between the sample and substrate. The platform was then placed inside the chamber and the device was switched on for 4.5 minutes, with an acceleration time of approximately 30 seconds.

1 L of the filtered spinning buffer (2mM dextrose in PBS) was dispensed into the spinning device chamber. The speed of the device was adjusted based on preliminary experiments to optimize detachment profiles; however it must be noted that the adhesion strength is independent of singular speed. Cells that were adhered to the samples for 1 hr were spun at 3000 revolution per minute (rpm) in order to detach them from the collagen surface. If seeding time was four hours or more, the speed was increased to 5000 rpm.

Once the spinning process was complete, samples were immediately taken off the platform and placed in a cytoskeleton (CSK)–Triton X-100 buffer for 10 minutes to puncture holes in the cells and stabilize their cytoskeletons. The cytoskeleton buffer (pH 6.8) was prepared with 3 mM MgCl₂, 50 mM sodium chloride, 10 mM PIPES buffer, and 0.15 mM sucrose in the DI water and 0.5% Triton X-100 solution [72]. The CSK-Triton X-100 buffer was then aspirated off before the samples were fixed with 3.7%

formaldehyde solution for 5 minutes and placed in a blocking buffer (1% BSA in PBS) solution for a minimum of 1 hr. 200 μ L of Hoechst (1:500) – BSA solution was dispensed on Parafilm sheets in the form of drops. The fixed collagen samples were then placed on top of the drops, and left in the dark for 45 minutes to allow the stain to penetrate into the nucleus of the cells. Samples were rinsed three times with DI water and then mounted on slides for analyzing purposes.

The samples were examined using a motorized stage and an Eclipse Ti-U fluorescent microscope (Nikon Instruments, Melville, NY). Most samples were examined with a Circular Cell Count Macro and NIS-Elements Advanced Research Software (Nikon Instruments) designed to take 61 pictures at different locations of the sample. The program displays an excel file with the number of cells found at each location. These counts were analyzed using the sigmoid adhesion fit created in the SigmaPlot 11 Program (Systat Software, San Jose, CA). It must be noted that some of the adhesion experiments were analyzed with Final Circular Cell Count – AnaRioja2012 Macro designed in the NIS-Elements AR Software due to software issues with the Circular Cell Count Macro. However, the only difference between the two macros is that the Final Circular Cells Count – AnaRioja2012 Macro takes 45 images from different locations of the sample instead of 61. These differences do not affect the results of the experiments; the only restraint is that cell seeding must be more accurate when using the 45 image macro in order to get good results.

2.7 Cell Spreading Area and Morphology

Fibroblasts were seeded on the four types of collagen samples and left inside the incubator for 4 hr to allow them to adhere to the surface. Cells were placed for 45 minutes in a CellTracker Green CMFDA fluorescent solution made of 25 μ L CMFDA and 12 mL DMEM, to permit the solution to penetrate the cell membranes. Once inside the cell, CMFDA is converted to a membrane impermeable fluorescent product. Spreading area quantification and shape analysis was done using the NIS-Elements Advanced Research Software (Nikon Instruments). At least four images per sample were taken; the images were taken at the same locations around the center of each sample. Approximately 200 cells were analyzed per sample.

2.8 Cell Migration Experiments

All four types of collagen substrates were cleaned and sterilized with ethyl alcohol (200 proof) and DPBS and placed inside 35mm TCDs (5 minutes with each solution). Scienceware Polystyrene Cloning Cylinders (6.4 mm diameter), purchased from Thermo Fisher Scientific Inc, were placed on top of the collagen samples. Approximately 33,437 cells were seeded in each cylinder and placed inside the incubator at 37°C for 24 hours to allow fibroblasts to adhere and form a uniform monolayer. The number of cells needed for these experiments was determined by calculating the ratio of number of cells needed per area, this ratio was based on Kondo et al.'s protocol [68].

$$\frac{1,000,000 \text{ cells}}{926 \text{ mm}^2} * 32.17 \text{ mm}^2 = 33,437 \text{ cells}$$

The cylinder was then removed and rinsed with DPBS to remove any cells that did not adhere to the surface. 2mL of complete growth media was added to each sample and taken to the Eclipse Ti-U fluorescent microscope (Nikon Instruments, Melville, NY) for analysis. By using the motorized stage and an image stitching program developed in the ND Sequence Acquisition, a 14 by 13 mm compilation picture was taken (shown below in Figure 22).

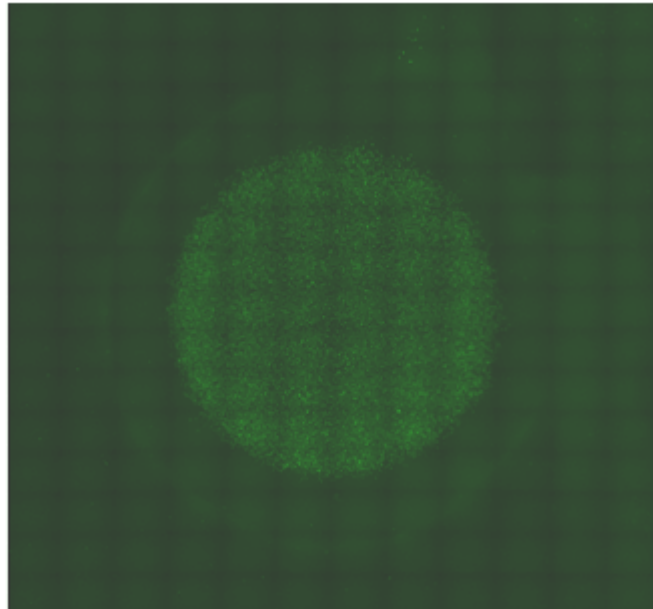


Figure 22 Stitching image of fibroblasts on a *wet* cross-linked surface taken immediately after fence removal.

The radius was found with the NIS Elements program: once three points were selected around the circumference of the circle, the program automatically drew a circle around the cells and calculated its radius. After the images were taken, the samples were returned to the incubator and left there for an additional 24 hours. Samples were taken again to the microscope in order to acquire the stitching images and the radius of each circle.

It must be noted that in the first few experiments, cells were stained with CellTracker Green CMFDA to ease the visibility of the cells on the surface from the stitching image. Soon after, it was found that cells did not need to be stained with this CellTracker because there was enough contrast between the cells and the substrates, especially when zooming into the image. The radius of each image was compared to determine the distance the cells traveled within the 24 hour period. By doing so, cell migration speed was determined for each of the four collagen sample and plain glass cover slips. Three to five different experiments were done per surface type.

CHAPTER 3: RESULTS

3.1 Optical Density (O.D.) vs. Wavelength of Collagen Networks

The graph shown below compares optical density between 800 μ L native and NDGA cross-linked samples. This volume was chosen since migration, adhesion, and spreading studies were done on gels containing this collagen volume.

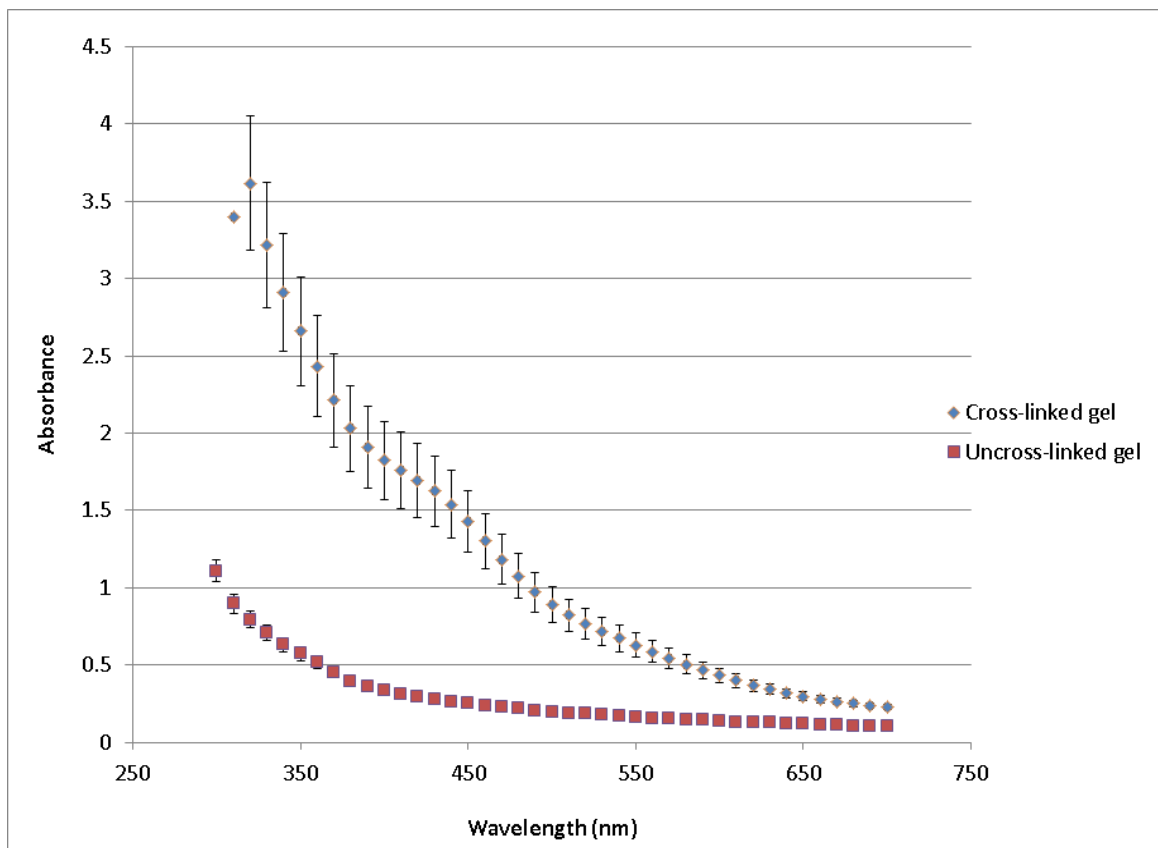


Figure 23 Absorbance of native and cross-linked collagen networks. An absorbance peak can be observed at approximately 420 nm, which indicates that collagen gel has been properly cross-linked with the NDGA solution. (N=5)

The absorbance peak observed around 420 nm indicates NDGA cross-linking within the collagen gel. This peak is not present in the uncross-linked collagen gel data. The graphs represent the average of five different measurements; the standard deviation was also calculated based on the data of these five samples. These results have been corroborated with studies performed by MiMedx Inc (*not shown*).

3.2 Collagen Gel/Film Thickness Measurements

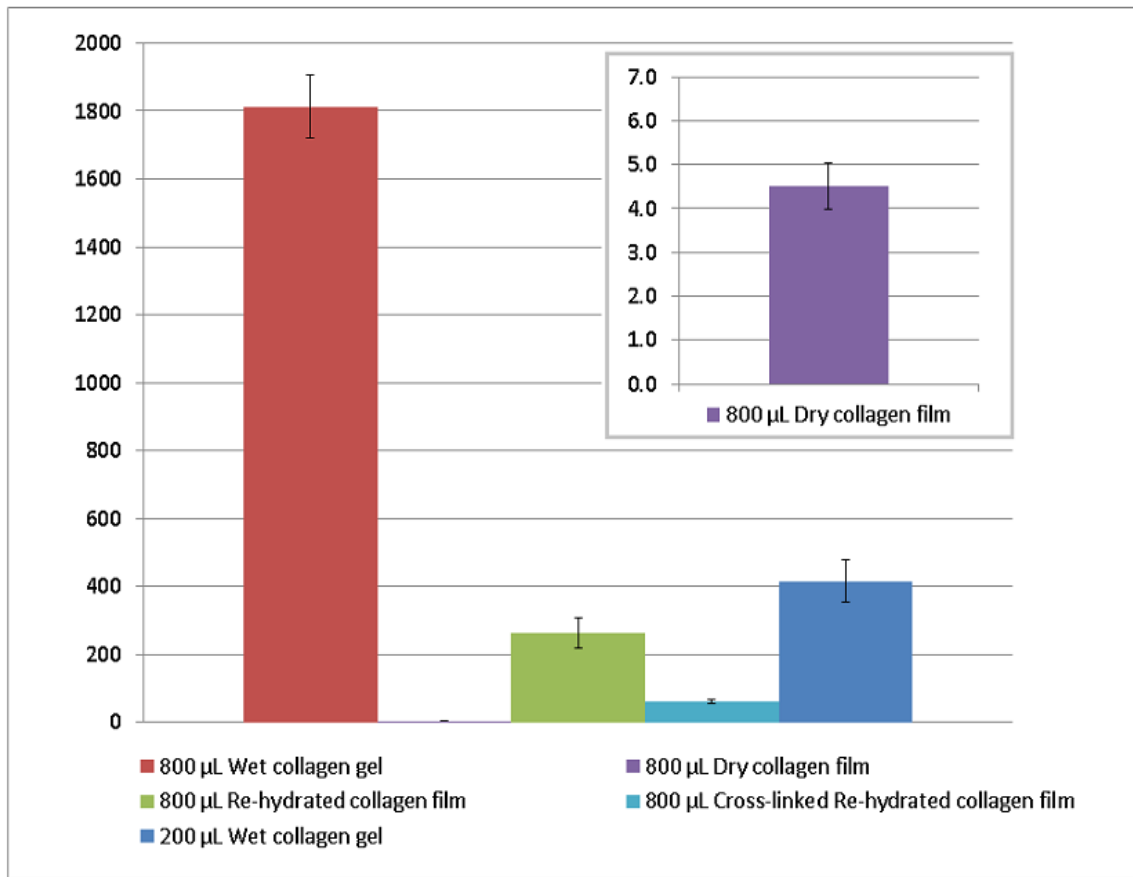


Figure 24 Thickness of collagen samples using different measuring techniques (N = 3). The thickness of the 800µL collagen gel decreases drastically once it dries out and becomes a film. The thickness is partially recovered once the 800µL film is rehydrated but decreases again after being cross-linked and *re-hydrated* once again. There is a statistical significance between each sample $P < 0.05$.

Thickness measurements were calculated using three techniques: contact angle camera, contact profiler, and optical profiler. The results of the thickness of each sample are shown above. The thickness of the collagen samples (except for the 800 μ L *dry* collagen samples) was quantified using pictures taken with the side-view camera on a contact angle measurement system. The average thickness of the 200 μ L *wet* collagen gels was found to be 416 μ m (\pm 62 SEM) while the average thickness of the 800 μ L *wet* collagen gels was discovered to be 1813 μ m (\pm 95 SEM).

After the 800 μ L *wet* collagen gels were dried, these films were washed with ethanol and left in PBS for at least one hour, the thickness of the *re-hydrated* film was then estimated to be 262 μ m (\pm 44 SEM). The average thickness of the cross-linked *re-hydrated* samples was found to be 63 μ m (\pm 5 SEM). These samples were prepared by cross-linking the *dry* films with NDGA and then re-hydrating them with PBS once the films were completely dried.

The contact and optical profilers were employed to measure the *dry* films. Both techniques measure the difference (step-change) between the collagen sample and the glass substrate. Half of the collagen was removed from each sample in order for the profilers to identify the height difference. The thickness measurements of the 800 μ L *dry* collagen samples were done with both techniques and averaged (8 points, 3 samples). The average thickness of the 800 μ L *dry* collagen film was found to be approximately 4.5 μ m (\pm 0.5 SEM). T-tests ($\alpha = 0.05$) confirmed there was a significant difference between these and the average thickness of the 800 μ L *re-hydrated* collagen films (262 μ m \pm 44 SEM).

3.3 Cell Adhesion Strength Experiments

Cell adhesion strength on collagen gels and films was determined using a spinning disk device, which applies a linear range of forces for detachment under constant and uniform chemical conditions at the surface [45].

3.3.1 Temporal Studies of Adhesion Strength

Figure 25 shown below displays the adhesion strength of cells adhered to 200 μ L *wet* collagen gels for different periods of times (incubation time). The graph shows an increase in adhesion strength from 1hr to 4hr, reaching steady-state at the 4 hr incubation time. At least 3 different experiments were completed to construct this graph.

A simple exponential curve was used to fit the adhesion strength versus seeding time data of both 200 μ L gels and 800 μ L uncross-linked films. This same fit has been utilized by others, such as Gallant et al [72]. A minimum of 3 experiments were done for each time point to assure that results were representative.

Statistical analysis was calculated between each time point to determine that adhesion strength reached steady-state at 4hr. No statistical significant difference ($P=0.065$) was found between the adhesion strength at 4hr ($597 \text{ dyne/cm}^2 \pm 37 \text{ SEM}$) and 24hr ($503 \text{ dyne/cm}^2 \pm 27 \text{ SEM}$). On the other hand, at 1hr the adhesion strength ($297 \text{ dyne/cm}^2 \pm 43 \text{ SEM}$) was found to be lower than the 4 hr time point demonstrating that adhesion strength keeps increasing between these two time points ($P \leq 0.001$).

Temporal adhesion studies were also done on 800 μ L collagen films. The result of this study is shown below. The adhesion strength of the cells on this sample also

increased from 1hr ($249 \text{ dyne/cm}^2 \pm 36 \text{ SEM}$) to 4hr ($554 \text{ dyne/cm}^2 \pm 23 \text{ SEM}$) showing that there is a statistical significant difference between the two time points ($P \leq 0.001$).

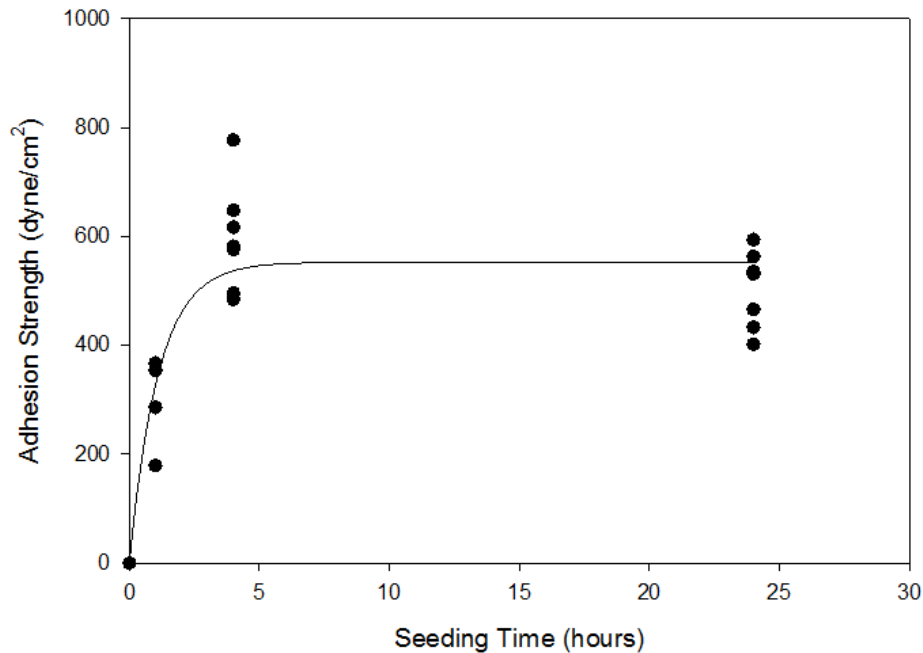


Figure 25 Temporal studies of adhesion strength for NIH 3T3 on 200 μ L collagen gels ($N \geq 4$). Adhesion strength increases from 1 hr to 4hr and reaches steady-state at 4hr ($R^2 = 0.73$).

The adhesion strength of the cells at 24hr was found to be $503 \text{ dyne/cm}^2 \pm 14 \text{ SEM}$) demonstrating that there is no statistical difference ($P = 0.087$) between this time point and the 4hr time point. Therefore, the steady-state of this sample was also reached at the 4 hr time point. These results are similar to observations that fibroblasts reach steady state adhesion on fibronectin-coated surfaces [72]. Based on these results, steady state adhesion strength was quantified on control and uncross-linked collagen gels and films.

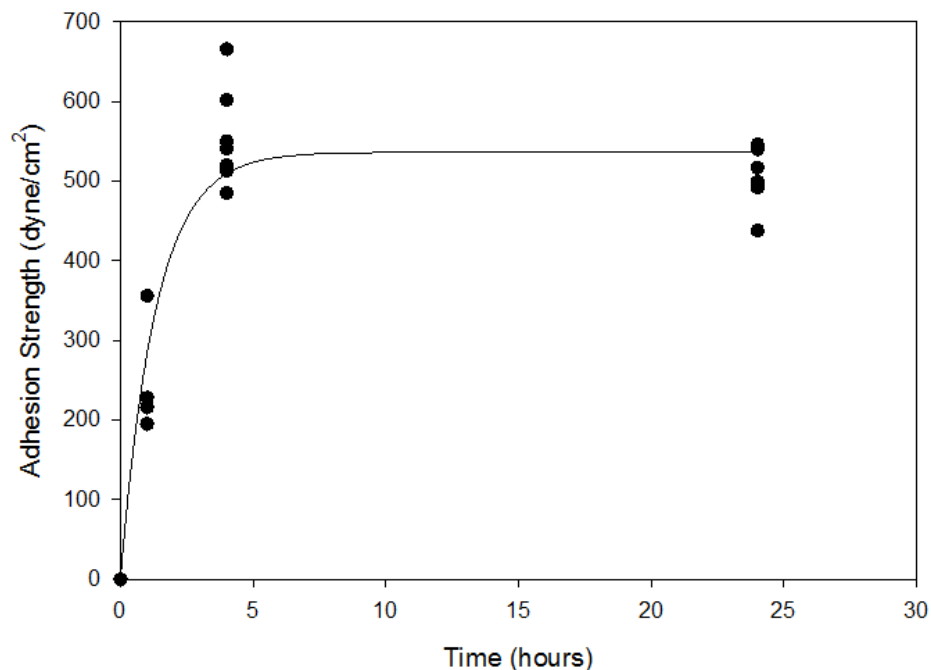


Figure 26 Temporal studies of adhesion strength for NIH 3T3 on 800 μ L collagen films ($N \geq 4$). Adhesion strength once again increases from 1 hr to 4 hr and then reaches steady-state at that time point ($R^2 = 0.85$).

3.3.2 Comparison of Adhesion Strength between *Wet Gels, Dry, Native, and Cross-Linked Films*

The mean adhesion strength of the 200 μ L gels was found to be 597 ± 37 dyne/cm² (uncross-linked) and 606 ± 25 dyne/cm² (cross-linked). No statistical significant difference in cell adhesion strength was found between the two 200 μ L samples ($P = 0.859$), or between uncross-linked collagen films and either cross-linked or uncross-linked collagen gels ($P > 0.05$). On the other hand, the t-test performed on the adhesion strength of the 800 μ L uncross-linked (554 ± 23 dyne/cm²) and cross-linked samples (456 ± 35 dyne/cm²) demonstrated a significant difference in adhesion strength between the samples ($P = 0.038$).

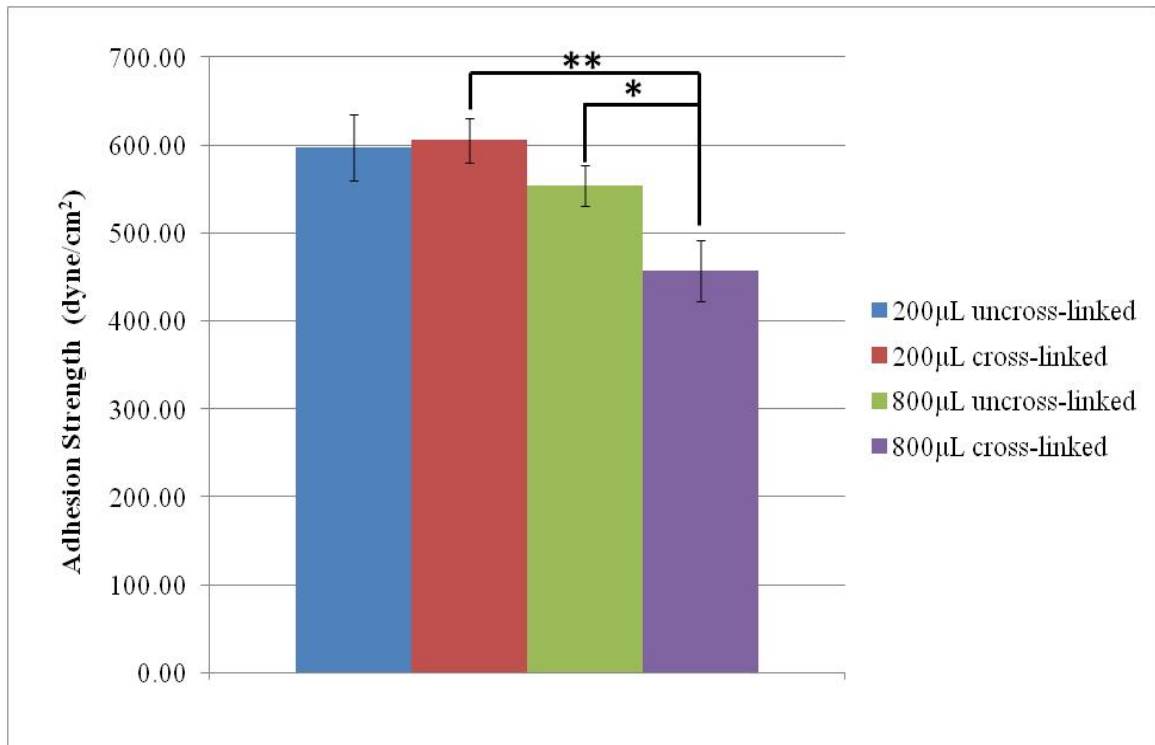


Figure 27 Adhesion data of fibroblast on *wet* (200µL) and *dry* (800µl) collagen gels (N ≥ 6). There is no statistical significance between 200µL uncross-linked and cross-linked gels. However, there is a difference between the 800µL uncross-linked and cross-linked films as well as between the 200µL cross-linked gels and 800µL cross-linked films. Statistical significance difference: P* < 0.05, P** < 0.01

In addition, there was a difference in the adhesion strength between cells that had been seeded on the cross-linked *wet* gels versus *dry* films that had been cross-linked (P = 0.006). At least three different adhesion experiments were performed for each sample, 6 to 9 data points of each sample were collected in order to graph Figure 27.

3.4 Spreading/Circularity Experiments

Cells were stained with the Green CellTracker dye prior to cell spreading and circularity analysis. Cells had been incubated on uncross-linked and cross-linked collagen gels for 4hr and 24hr.

3.4.1 Temporal Cell Spreading Studies on Cross-Linked and Native *Wet* Collagen Gels

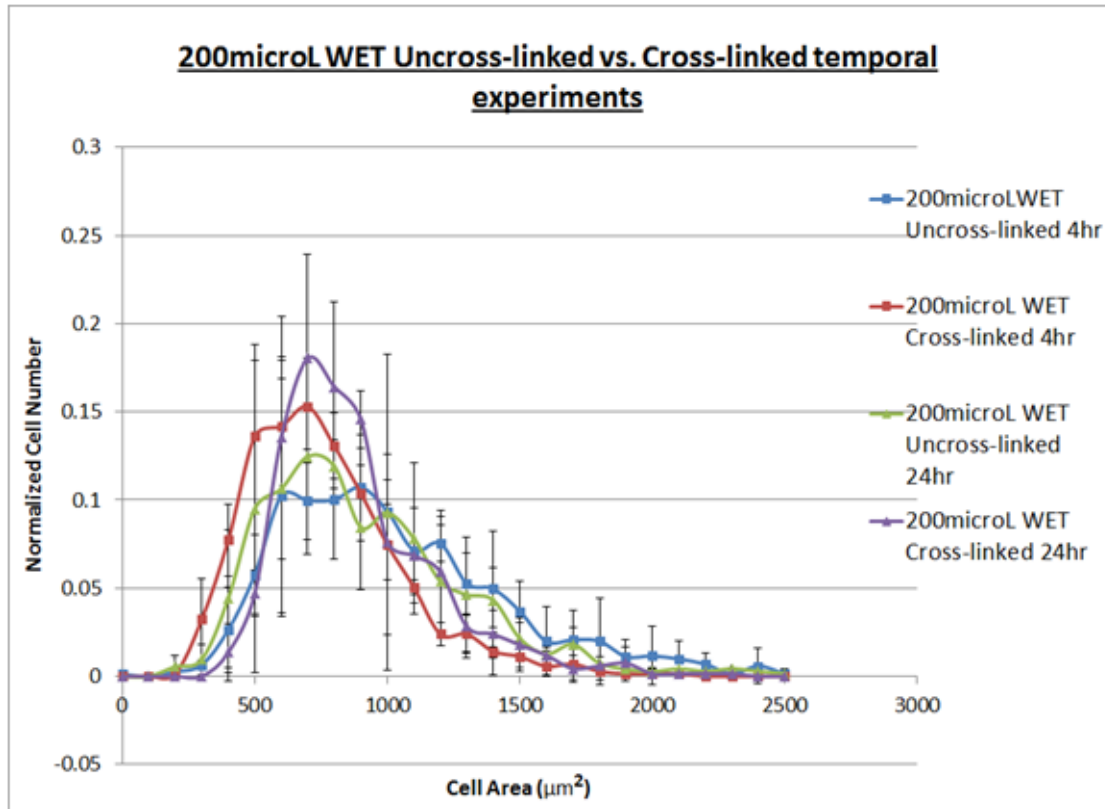


Figure 28 Cell spreading area of NIH 3T3 on 200 μL uncross-linked and cross-linked *wet* collagen gels at 4hr and 24hr (N = 3).

Each histogram was graphed with average points from three different sets of experiments (approximately 200 cells per experiment). Cell frequencies were normalized for direct comparisons between experiments and the standard deviations shown in the graph were calculated for each area bin. However, statistical comparisons of mean area were made by comparing the average cell area from three different experiments. The average cell spreading area of cells seeded for 4 hr on top of 200 μL uncross-linked collagen gels was calculated to be $985 \mu\text{m}^2 \pm 111 \text{ SEM}$, while at 24hr incubation time it was determined to be $892 \mu\text{m}^2 \pm 98 \text{ SEM}$. No significant difference in cell spreading

area was discovered by increasing the incubation time on uncross-linked samples ($P = 0.565$); this was also true on the cross-linked surfaces ($P = 0.211$) where the cell spreading area was found to be $728 \mu\text{m}^2 \pm 32 \text{ SEM}$ (4hr incubation time), and $843 \mu\text{m}^2 \pm 70$ (24hr incubation time). No significant difference was found between uncross-linked and cross-linked samples when being compared based on incubation times. A summary of the statistical analysis of these experiments is shown in the following diagram.

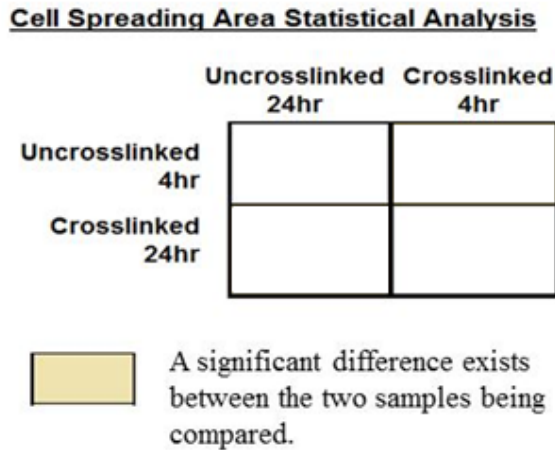


Figure 29 Statistical analysis of cell spreading area on 200 μL *wet* collagen gels.

3.4.2 Temporal Cell Circularity Studies on Cross-Linked and Native *Wet* Collagen Gels

As a measure of cell morphology, the shape parameter circularity (closeness to a circle; $=4\pi \cdot \text{area} / \text{perimeter}^2$) was also compared between these four samples. Average circularity was determined by the NIS Elements software from randomly selected cells (approximately 200 cells per experiment). The measure of circularity ranges from 0 to 1, where 1 describes a cell that is a perfect circle.

The average cell circularity for the 200 μL uncross-linked at 4hr incubation time was $0.50 \pm 0.04 \text{ SEM}$, while at 24hr incubation time was $0.57 \pm 0.08 \text{ SEM}$. No statistical

difference ($P = 0.130$) was determined between the two uncross-linked samples ($P = 0.486$) or between the cross-linked samples at distinct incubation periods (4hr: 0.63 ± 0.02 , and 24hr: 0.57 ± 0.02). Surprisingly, a significant statistical difference ($P = 0.046$) was discovered between the uncross-linked and cross-linked samples at the 4hr incubation time. However, no statistical significant difference was found between cells seeded on cross-linked and uncross-linked after the 24hr incubation time ($P = 0.942$).

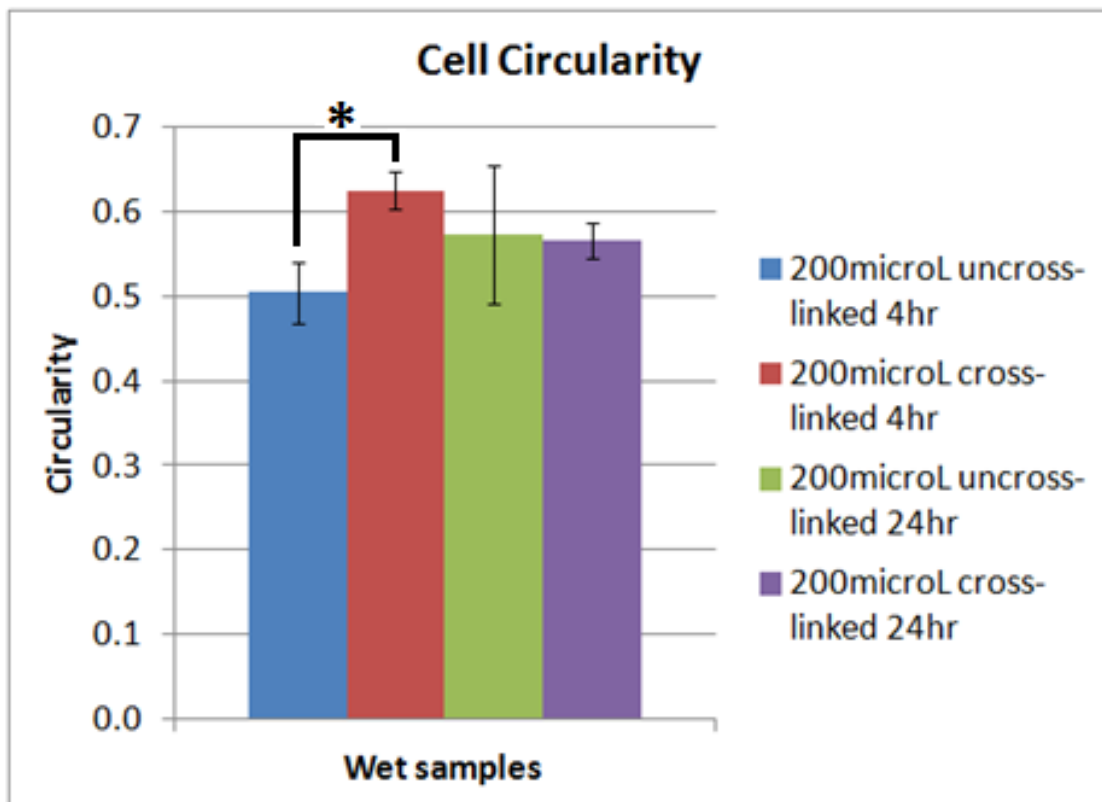


Figure 30 Cell circularity of NIH 3T3 on uncross-linked and cross-linked *wet* collagen gels at 4hr and 24hr. A difference in circularity is observed between the 200µL uncross-linked versus cross-linked samples. * indicates a significant difference ($P < 0.05$).

3.4.3 Temporal Cell Spreading Studies on Cross-Linked and Native *Re-hydrated* Collagen Films

The same temporal studies of cell spreading and morphology for uncross-linked and cross-linked collagen gels were done with the 800µL dried and rehydrated films.

Again it was found that there was no significant difference in spreading area of cells on 800 μ L films that underwent different incubation times. After a 4hr incubation time, cells on uncross-linked films had an average spreading area of 1049 $\mu\text{m}^2 \pm 11$ SEM, while the average spreading area of cells on those same samples at the 24hr incubation time was found to be 1047 $\mu\text{m}^2 \pm 81$ SEM ($P = 0.983$). Similarly no difference was observed between cells on cross-linked samples that had an average spreading area of 685 $\mu\text{m}^2 \pm 59$ (4hr incubation time) and the spreading area of cells that were left on the samples for a 24hr incubation time 753 $\mu\text{m}^2 \pm 57$ SEM ($P=0.453$).

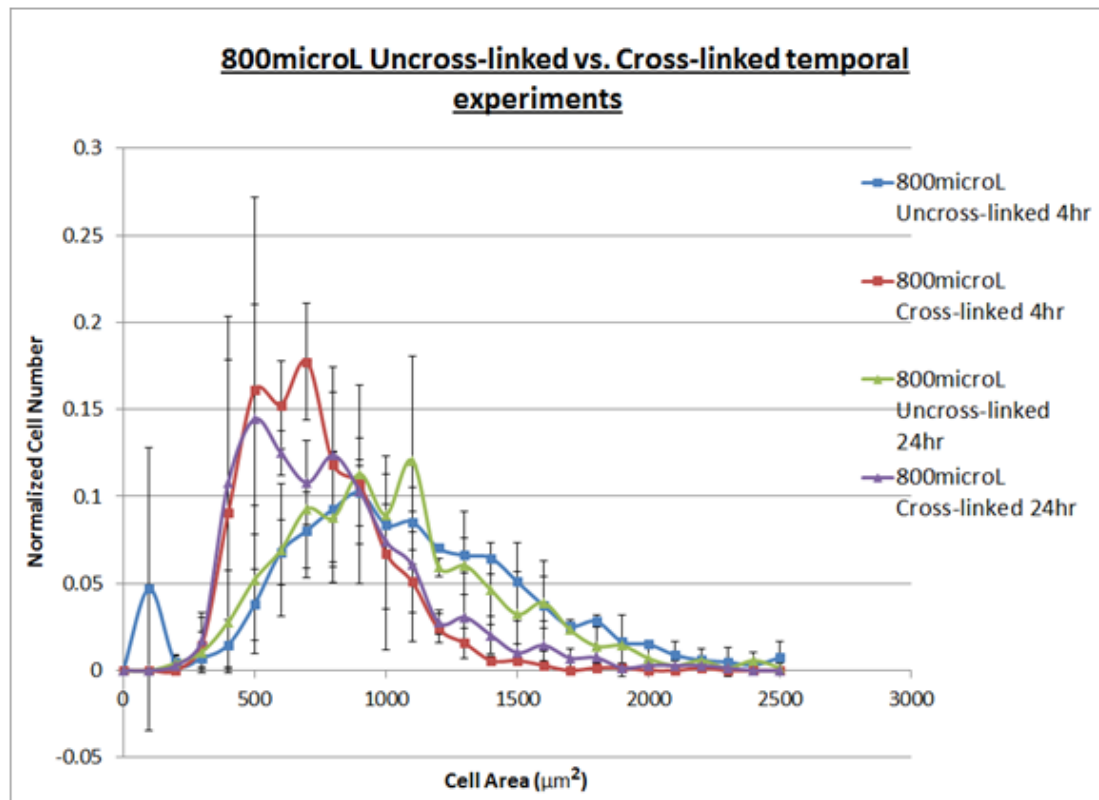


Figure 31 Cell spreading area of NIH 3T3 on 800 μ L uncross-linked and cross-linked *re-hydrated* collagen films at 4hr and 24hr (N = 3).

On the other hand, unlike the spreading area studies of cells on 200 μ L uncross-linked versus cross-linked which demonstrated that there was no difference between

these two samples, a clear difference was found between the cells seeded on uncross-linked and cross-linked 800 μ L samples at both 4hr ($P = 0.004$), and 24hr incubation periods ($P = 0.041$).

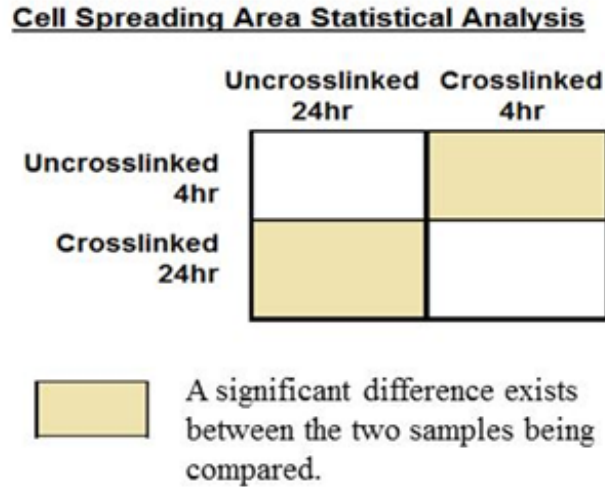


Figure 32 Statistical analysis of cell spreading area on 800 μ L *re-hydrated* collagen films.

The figure above illustrates whether there are statistical significant differences between the four samples. No difference exists between 4hr and 24hr spreading area experiments; however, a significant difference on cell spreading area between uncross-linked and cross-linked samples can be observed. All the statistical analysis was completed using the statistical functions of SigmaPlot 11.

3.4.4 Temporal Cell Circularity Studies on Cross-Linked and Native *Re-hydrated* Collagen Films

The circularity of the cells seeded on the four 800 μ L *re-hydrated* collagen surfaces was also investigated. Similar to the *wet* gel studies, a significant difference in cell circularity was observed between the cells on the dried film uncross-linked and cross-linked samples at the 4hr incubation time ($P = 0.008$). At 4hr, the average

circularity of the cells on top of 800 μ L uncross-linked films was 0.52 ± 0.03 SEM, while 0.67 ± 0.02 SEM was the average circularity of the cells seeded on the cross-linked samples. However, this difference was no longer apparent at 24hr. Cells that went through a 24hr incubation time had an average circularity of 0.58 ± 0.07 (uncross-linked) and 0.59 ± 0.08 (cross-linked). No significant difference was found between these two samples ($P = 0.988$). There was also no significant difference in circularity between the cells that were seeded at 4hr versus 24hr on both uncross-linked ($P = 0.412$) and cross-linked samples ($P = 0.404$).

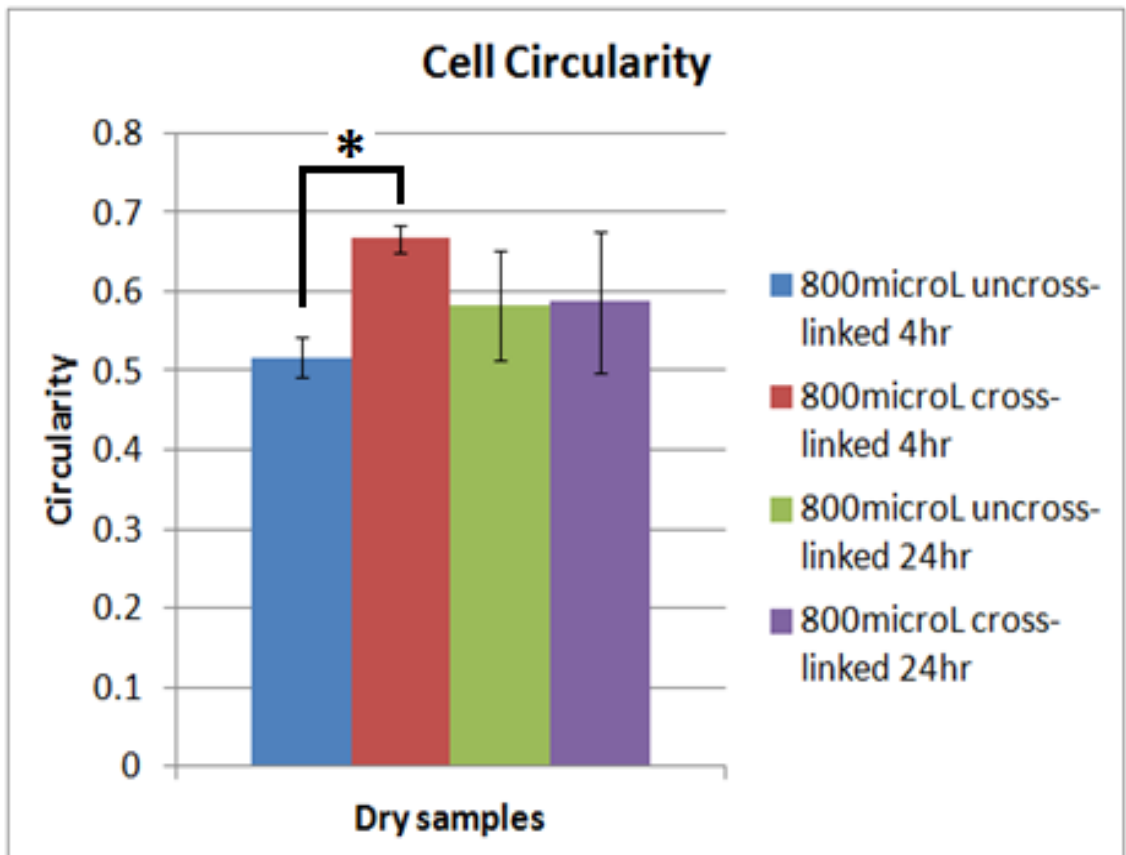


Figure 33 Cell circularity of NIH 3T3 on 800 μ L uncross-linked and cross-linked *dry* collagen films at 4hr and 24hr. Statistical significant difference: $P^* < .005$

3.5 Cell Migration Experiments

Migration was also studied on cells seeded on the four different collagen samples. The figure below shows an increase in cell coverage area due to migration, which is observed as radial expansion following the removal of a circular barrier.

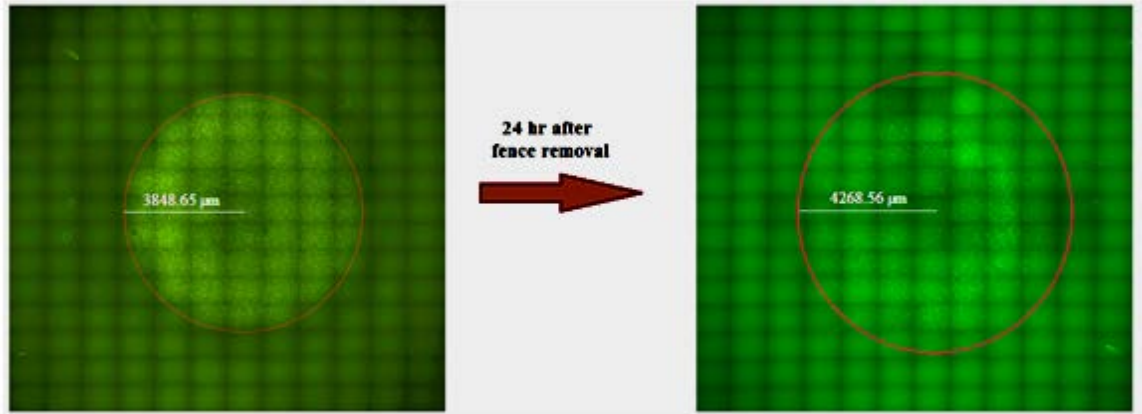


Figure 34 Analysis of 24 hours migration experiments (change in radius) with NIS Elements software.

The average radial migration speed in 24 hours was calculated by subtracting the radius of the circle from the image taken after 24hr fence removal minus the radius of the circle from the image taken as soon as the fence was removed from the sample, all divided by the 24hr time period.

$$\text{Avg. radial migration speed in 24 hr} = \frac{(\text{Final radius} - \text{Initial Radius})}{24 \text{ hours}} \quad (\text{Eq. 3})$$

An example calculation is shown below using data taken from the figures above.

$$\text{Avg. radial migration speed} = \frac{(4268.56 \mu\text{m} - 3848.65 \mu\text{m})}{24 \text{ hours}} = 17.50 \mu\text{m} * \text{hr}^{-1}$$

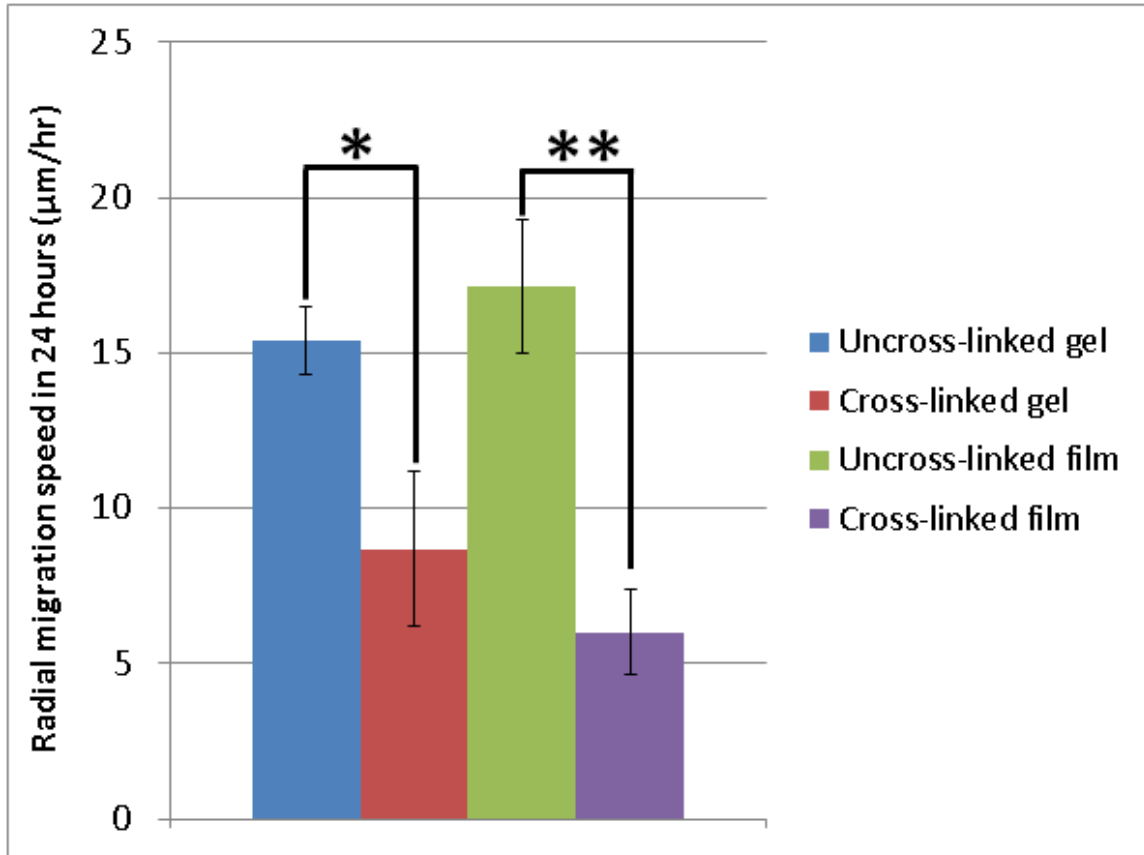


Figure 35 Average radial migration speed in 24 hours ($N \geq 8$). Statistical significance: $P^* < 0.05$, $P^{**} < 0.001$.

The average radial migration of the cells seeded on top of the 200µL cross-linked collagen gels ($8.70\mu\text{m} \pm 2.49$ SEM) was very similar to the one found from the cells residing on the 800µL cross-linked surface ($6.02\mu\text{m} \pm 1.38$ SEM), and there is no statistical significant difference between these two samples ($P = 0.362$). There was also no significant difference ($P = 0.492$) between the average radial speed travelled by the cells on the 200µL uncross-linked collagen gels ($15.39\mu\text{m} \pm 1.08$ SEM) and on the 800µL uncross-linked samples ($17.13\mu\text{m} \pm 2.16$ SEM).

Cells migrated faster on the 200µL uncross-linked surfaces than on the 200µL cross-linked ones ($P=0.017$). A similar difference was also observed when the cells on

the 800 μ L uncross-linked samples were compared to the ones seeded on the 800 μ L cross-linked surfaces ($P = 0.001$).

CHAPTER 4: DISCUSSION

Nordihydroguaiaretic acid (NDGA) has been demonstrated to be beneficial for many clinical applications. It does not only have anti-inflammatory capabilities, but it is also utilized in medicine to aid with the cure of various diseases such as diabetes and rheumatism. Due to all the benefits that have been discovered of this antioxidant extracted from the creosote bush, various studies are being conducted to learn more about the general properties of NDGA and its possible use in the clinical environment. [39]

Various scientists such as Koob et al. [40, 69, 70] and Ju et al. [73] have investigated for years and discovered that collagen materials treated with NDGA cross-linking solutions have higher tensile strength and enhanced compatibility when implanted in the body. *In-vivo* and *in-vitro* studies on other cross-linking agents such as glutaraldehyde and carbodiimide have been conducted to gain a better understanding of these materials; however, most of the NDGA-collagen biomaterials information has been gathered from animal studies (*in-vivo*).

These animal studies have been very useful for gaining a better understanding on the properties and advantages of this cross-linking agent on tendon replacement (biocompatibility, material with tendon-like strength). However, *in-vitro* studies will help us learn more about cellular behavior on this material, which is necessary to determine if the material would be ideal for implantation as a tendon replacement.

The goal of this thesis was to investigate whether cells seeded on NDGA cross-linked collagen samples would adhere and migrate on this collagen material. If adhesion and migration occurs, then it is expected that resident cells will be able to populate and regenerate the tendon and possibly reduce the immobilization time post-surgery.

This study is based on previous investigations done by Koob et al. [41, 69, 70] that focused on exploring the capabilities of NDGA collagen fibers for future tendon replacement; however, instead of fibers, gels and films were utilized to facilitate cell adhesion analysis. Thus despite the difference in geometry between the flat gels/films described here, there are comparable to the extruded fibers typically used for tendon replacement products. An optical density' analysis of the native and NDGA cross-linked samples was done to demonstrate that this biomaterial was manufactured with the same constituents and protocols utilized to make NDGA collagen fibers. The absorbance peak discovered at approximately 420 nm of the wavelength was compared to the one found by MiMedx Inc (*data not shown*) indicating that the material utilized for the studies described in Chapter 3 was the same one employed by Koob et al [41, 69, 70].

It has been discovered that a surface must have a certain thickness in order for cells to sense the material; however, a specific sensing thickness value has not been found. Some scientists suggest that this value is approximately 100 μ m [74], while others estimated it to be much smaller [75]. Based on these studies, it was determined that the collagen gel and film' thickness should be greater than 50microns, not only to avoid cells from sensing the underlying substrate but also to approximate the size of the fibers that MiMedx Inc. is manufacturing.

Since both gels and *re-hydrated* films are *wet*, the contact angle camera was employed to determine the thickness of the both uncross-linked and cross-linked gels and films (details described in Chapter 2). The measurements done by this equipment were corroborated by the calculations of the 800 μ L gels shown below.

$$\mathbf{Area}_{cover-slip} = \pi * r^2 = \pi * \left(\frac{25mm}{2}\right)^2 \approx \mathbf{491 mm^2} \quad (\text{Eq. 4})$$

$$\mathbf{Thickness}_{gel} = \frac{\mathbf{Volume of collagen}}{\mathbf{Area of cover-slip}} \quad (\text{Eq. 5})$$

$$\mathbf{Thickness}_{gel} = \frac{800\mu L}{491 mm^2} = \frac{0.8 mL}{491 mm^2} * \frac{1000 mm^3}{1 mL} \cong \mathbf{1.63mm}$$

The thickness measurements found for both 200 μ L and 800 μ L collagen gels were similar to the ones calculated. Therefore, all the film measurements done with this machine were considered to be accurate. An 85.5% thickness reduction between 800 μ L *wet* gels and *re-hydrated* films was observed. This drop in thickness is not surprising since approximately 90% of the collagen volume was reduced due to water loss (change in weight before (gel) and after the drying process (film)). Cross-linking of the films was found to cause an even bigger reduction in film thickness (96.5%).

NDGA fibers manufactured by MiMedx Inc. were found to rebound approximately 60% in diameter after they had been cross-linked and *re-hydrated* the second time (Personal communication with Dr. Thomas J. Koob). However, thickness

results demonstrate that our films do not have a similar rebound percentage which could be due to the geometry of the sample. Fibers are able to re-hydrate themselves and increase in volume in all radial directions; on the other hand, gels and films are only able to increase their volume in a single direction.

Once the measurements for both gels and films were proven to be thicker than 50 microns, cell studies were performed to determine if cell behavior was affected by the cross-linking treatment of the collagen samples. Collagen gels (200 μ L) were manufactured and cross-linked with the NDGA solution based on an adaptation from the protocol designed by Koob et al [41]. Once these *in-vitro* platforms were manufactured, NIH 3T3 cells were seeded on these surfaces to determine whether cell behaviors on collagen materials were affected by NDGA cross-linking.

Prior to seeding the cells on these platforms, the 200 μ L cross-linked collagen gels were treated with ethanol and UV light for sterilization purposes. Past studies determined that the extent of UV light exposure to a sample not only affects the cross-linking of the collagen surface but also tends to fragment the collagen triple helical formation [20]. For this reason, the 800 μ L samples that were dried and *re-hydrated* before and after cross-linking (same procedure utilized by MiMedx to manufacture the collagen fibers [41]) were only sterilized with ethanol. These films did not undergo any UV treatment in order to avoid changes in the material properties.

Previous adhesion studies have demonstrated that the strengthening kinetics of NIH 3T3 fibroblasts on fibronectin leads to rapid enhancement of adhesion strength at early seeding time points and saturation being reached at the 4hr time period [45]. Temporal adhesion studies were done to corroborate that fibroblast adhesion strength

reached steady-state at the 4hr time period on both 200 μ L collagen gels and 800 μ L films. The temporal studies of both 200 μ L gels and 800 μ L films demonstrated that cellular adhesion strength did not increase between the 4hr and 24hr seeding period. Therefore, additional adhesion studies of cells seeded on all the four different samples (200 μ L uncross-linked gel, 200 μ L cross-linked gel, 800 μ L uncross-linked film, and 800 μ L cross-linked film) were only done at the 4 hour time point.

Although temporal adhesion experiments demonstrated that cells reach steady-state at 4hr, it was also investigated whether cell spreading varied from 4hr to 24hr; it was observed that no difference exists in cell spreading between these two time points. The results of the temporal cell spreading area support the temporal adhesion strength experiments, demonstrating that by 4 hours cells stop spreading on the collagen surfaces and their strength to adhere to these surface reaches steady-state.

Cells that were seeded on both 200 μ L uncross-linked and cross-linked gels did not have a statistical significant difference in adhesion strength (1.5% difference) or cell spreading area (26.1% difference at 4hr, and 5.6% difference at 24hr). These observations lead to the hypothesis that cross-linking did not alter fibroblast behavior. However, 24hr radial migration studies between the uncross-linked and cross-linked surfaces demonstrated that cell behavior was definitely affected by a significant 43.5% reduction in migration speed for cells residing on the NDGA cross-linked collagen gels.

These conflicting results, however, were not consistent with our studies of adhesion and migration on gels that had be dried into films and then partially *re-hydrated*. When analyzing the cellular studies done on the 800 μ L collagen films, a difference was not only found in migration studies but also in adhesion strength and

spreading area studies. A 17.7% reduction in adhesion strength was discovered between cells seeded on uncross-linked versus cross-linked samples. A decrease in cell spreading area was also found on cells residing on the cross-linked surfaces at both 4hr (34.7%) and 24hr incubation time (28.1%). Similar to the results of the migration studies done on the 200 μ L gels, a difference in speed was also discovered in the 24hr migration studies of the 800 μ L films. However, the reduction in the cell's speed (64.9%) on the cross-linked films was larger than the one found for the cells residing on the cross-linked gels; although no statistical significant difference exists between the two values.

No significant difference was found between the average cell spreading area of the cells seeded on the uncross-linked and cross-linked collagen gels or between the adhesion strength of the cells residing on the two different samples. On the other hand, a difference in cell spreading area between the cells located on uncross-linked versus cross-linked films also agree with a difference found in their adhesion strength. These observations demonstrate a possible correlation between adhesion strength and spreading area analysis. This correlation is supported by the findings acquired by others studies [52] that state that cells with higher spreading areas remain attach to the surface for longer periods of time and have higher adhesion strength.

Cell spreading and migration are both multistep processes that strongly depend on adhesion strength for proper functionality. Various studies, including the one done by Palecek et al. [61] have been accomplished to gain a better understanding on how adhesion strength and biochemical modifications of anchoring sites alter migration speed. This group found a correlation between cell migration speed and cell-substrate

adhesiveness, which depend in various factors such as extracellular matrix (ECM) concentration and integrin expression. [61]

Even though studies of ECM concentration and integrin expression were not done in this thesis, adhesion strength measurements, which are direct quantifications of cell-substrate adhesiveness, were performed and compared to cell migration studies. No correlation was observed between cell-substrate adhesiveness and cell migration speed of the fibroblasts on the 200 μ L collagen gel studies. On the other hand, a correlation between these two variables was discovered in the 800 μ L collagen films' studies.

DiMilla et al stated that the spreading area of a cell or its adhesiveness is related to its migration rate; however, the relationship is biphasic. Cells that are weakly adhered to a surface won't be able to migrate because of the lack of traction forces necessary for migration. At the same time, cells that are too strongly attached to the surface augmenting the bonds between the cell and the surface and limiting the possibility of migration. [60]

The adhesion, spreading, and migration studies of the 800 μ L films support the observation described by DiMilla. However, it is difficult to understand why even though there are no differences in cells spreading area and adhesion strength between the 200 μ L uncross-linked and cross-linked samples, a difference in cell migration speed does exist between these two samples.

Fibroblasts that are seeded on a surface tend to have a circular shape, and as they begin spreading they become elongated and less circular. Therefore, it is interesting to find a difference in cell circularity on cells seeded for 4hr on uncross-linked versus cross-linked films (22.4% difference) since a reduction in spreading area was not only observed on 800 μ L cross-linked films at 4hr but also at the 24hr incubation time. Circularity values

of cells residing on uncross-linked versus cross-linked gels were also significantly different (20.6% difference) at the 4hr incubation time; however, no statistical difference was found between the spreading areas values of cells placed atop of the two types of 200 μ L gels.

Cellular analysis of the 200 μ L uncross-linked gels versus the 800 μ L uncross-linked films was also compared; no difference was found in adhesion strength, cell spreading area, cell circularity, or cell migration studies. Consequently, it is interesting that a difference in adhesion strength and spreading area does exist between 800 μ L uncross-linked and cross-linked films but not between uncross-linked and cross-linked gels.

At first, the NDGA treatment on collagen was considered to be a complete polymerization technique [70]; however, recent studies done by MiMedx Inc. (Personalized communication with Dr. Thomas J. Koob) have demonstrated that chemical cross-linking is likely also occurring when the NDGA solution is added onto the collagen substrates. It is hypothesized that this cross-linking takes place when the collagen's amino acids, arginine and lysine, react with the NDGA compound.

Based on our observations and the ones gathered from MiMedx Inc., we believe that the drying process employed to make the films is the reason why a difference in cell behavior exists between gels and films. Collagen gels begin to dry and start to collapse forming films; however, this does not occur in the swollen gels. Therefore, we hypothesize that this collapse makes the substrate denser; pushing the collagen fibers closer to each other possibly promoting an interaction between them and allowing for the available shorter links of the NDGA to more extensively cross-link to the collagen

networks. This natural cross-linking between the collagen fibers within the film and with NDGA may reduce the amount of NDGA polymerization required to enhance the tensile properties of the material. On the other hand, gels that are always *wet* may not be able to form as many collagen links with themselves and with NDGA since they lack the necessary proximity for natural cross-linking to occur.

Consequently, we also hypothesize that the reason there is a difference between uncross-linked and cross-linked films is that NDGA treatment could be masking the cell receptor binding sites either physically, chemically, or both. Without the necessary binding sites, cells are not able to adhere as strongly to a surface and resist detachment forces. NDGA may also be taking up chemical residues necessary for cells to adhere to these films affecting the cellular behavior.

Although adhesion, spreading, and migration is lower for fibroblasts seeded on top of cross-linked films, the reduction is not an impediment for this biomaterial to be used as a tendon replacement. This is especially true since other cross-linking solutions such as carbodiimide, which does not provide the same tensile strength as NDGA, also demonstrate that the cell spreading area is reduced when cells are seeded on the cross-linked surfaces [76].

This study was able to determine that cells are able to migrate and adhere to the NDGA cross-linked collagen surfaces, which is necessary for recruitment of other cells for faster tendon regeneration. And even though the investigation was focused on collagen films as opposed to fibers; these results bring support to the idea that cells will also migrate and proliferate in the fibers since the same protocol and components were utilized to create both NDGA-collagen biomaterials.

CHAPTER 5: CONCLUSIONS AND FUTURE WORK

NDGA cross-linking on collagen materials has been studied by others due to its various advantages such as biocompatibility, biodegradability, and enhancement of tensile strength [40, 69, 70, 73]. Although other cross-linking approaches (e.g. carbodiimide and glutaraldehyde) also augment the tensile strength of collagen materials, the increase in this strength is not comparable to the degree of enhancement achieved with the NDGA treatment.

The results of this study demonstrate that NDGA cross-linking affects cell behavior (cell spreading and adhesion) on collagen films but not on gels. We hypothesize that the difference in cell behavior only exists on the films because of the collapsing that occurs in the collagen gel once it is completely dried. Observations by MiMedx Inc. support our hypothesis that this collapsing allows the collagen fibers to naturally begin to cross-link with each other and with the NDGA solution. On the other hand, NDGA treatment of gels may be mostly due to polymerization instead of cross-linking, since collagen fibers are located farther apart in the swollen gels.

Cross-linkers such as glutaraldehyde employ both polymerization and cross-linking; however, it has been discovered that cross-linking occurs at a faster rate than polymerization, and for this reason glutaraldehyde treatment is mostly considered a cross-linking technique. Based on our studies, we have determined that NDGA treatment also

utilizes both cross-linking and polymerization techniques to enhance tensile strength of the material.

The difference in cell behavior may exist because NDGA treatment of the collagen samples could be masking possible adhesion sites necessary for cells to strongly adhere to these substrates. The masking could be either physically (NDGA polymerization), chemically (NDGA- collagen and collagen-collagen cross-linking), or both. NDGA cross-linking, which we hypothesize is mostly happening in the films may be affecting cell behavior more than NDGA polymerization which we believe is mostly occurring in the gels. This is hypothesized since cell adhesion strength and spreading area between 200 μ L uncross-linked and cross-linked samples were not affected by the NDGA polymerization.

It is believed that the NDGA treatment of these gels is mostly based on polymerization than on cross-linking since the swollen gels do not provide enough proximity for natural cross-linking (collagen-collagen interaction) to occur. On the other hand, collapsed collagen films could have the necessary proximity for cross-linking to occur at a faster rate than polymerization affecting the behavior of the cells residing on top of this surface.

Even though NDGA cross-linking affects cell behavior, this effect is not tremendous enough to eliminate the possibility of the employment of this biomaterial in implantation purposes (i.e. tendon replacement). This is especially true since it has been demonstrated that other cross-linking solutions, such as carbodiimide, that have fewer benefits than NDGA also show that cell spreading area is reduced on their cross-linked surfaces.

Based on all the results found in this study, we can be concluded that NDGA cross-linked biomaterials are likely to be appropriate for future tendon implantations. However, other studies should be done to provide additional support to this idea.

First, the extent of NDGA cross-linking should be investigated by amino acid analysis on both formed gels and *re-hydrated* films to determine the difference in available lysine residues. We expect to find a greater reduction in free lysine residues on the collagen films than on the gels which would support the idea that more NDGA cross-linking is occurring on the films via amine groups in lysine residues. This experiment will also help us understand whether binding is occurring mostly with the collagen fibers themselves or with the NDGA solution. ELISA testing should also be done to determine the number of available receptor binding sites on these four different collagen surfaces. These two experiments will help us determine if NDGA treatment is masking the adhesion sites physically, chemically, or both.

Gallant et al [72] demonstrated that integrin binding and the formation of focal adhesion complexes are the two main factors that provide mechanical strength for attaching to materials. A reduction in either factor reduces the adhesion strength between the cell and its surface. Therefore, the next experiment will be focused on quantifying the number of integrins bound in the surface as well as the recruitment of focal adhesion proteins. By doing this, we will be able to gain a mechanistic understanding of why cells residing on the 800 μ L NDGA cross-linked films have lower adhesion strength than the ones seeded on the 800 μ L uncross-linked films. Techniques such as the wet-cleaving assay described by Michael et al. [53], will provide the necessary information to determine the distribution of focal adhesion areas and bound integrins within the areas of

adhesion. By utilizing this technique, the difference in the number of bound integrins and focal adhesion proteins found on the uncross-linked and cross-linked films will be determined.

Lastly, understanding cell interactions with collagen-based biomaterials is of fundamental importance since collagen is the most abundant protein in the body and is found in nearly all tissues including the skin, ligaments, and bones. The *in-vitro* platforms (collagen gels and films) developed in this work could be utilized to investigate the behavior of different cell types on collagen materials with varied properties, broadening their use to other tissue engineering and biomaterials applications.

REFERENCES

1. Amiel, D., E. Billings, and W.H. Akeson, *Ligament structure, chemistry, and physiology*. Knee Ligaments: Structure, Function, Injury, and Repair. 1990, New York: Raven Press 77-91.
2. *Tendon Injuries: Basic Science and Clinical Medicine* N. Maffulli, P. Renstrom, and W.B. Leadbetter, Editors. 2005, Springer: London.
3. Jozsa, L. and P. Kannus, *Human Tendons: Anatomy, Physiology, and Pathology*. Human Kinetics. 1997, Champaign, IL.
4. Oxlund, H., *Relationships between the biomechanical properties, composition and molecular structure of connective tissues*. Connect Tissue Res, 1986. **15**(1-2): p. 65-72.
5. Gray, H. and W.H. Lewis, *Anatomy of the human body*. 20th ed. 1918, Philadelphia and New York,: Lea & Febiger.
6. Strickland, J.W., *Development of flexor tendon surgery: twenty-five years of progress*. J Hand Surg Am, 2000. **25**(2): p. 214-35.
7. Koob, T.J., *Biomimetic approaches to tendon repair*. Comp Biochem Physiol A Mol Integr Physiol, 2002. **133**(4): p. 1171-92.
8. Banes, A.J., et al., *PDGF-BB, IGF-I and mechanical load stimulate DNA synthesis in avian tendon fibroblasts in vitro*. J Biomech, 1995. **28**(12): p. 1505-13.
9. Hannafin, J.A., et al., *Effect of stress deprivation and cyclic tensile loading on the material and morphologic properties of canine flexor digitorum profundus tendon: an in vitro study*. J Orthop Res, 1995. **13**(6): p. 907-14.
10. Malaviya, P., et al., *An in vivo model for load-modulated remodeling in the rabbit flexor tendon*. J Orthop Res, 2000. **18**(1): p. 116-25.
11. Woo, S.L., et al., *The effects of exercise on the biomechanical and biochemical properties of swine digital flexor tendons*. J Biomech Eng, 1981. **103**(1): p. 51-6.

12. Banes, A.J., et al., *Gap junctions regulate responses of tendon cells ex vivo to mechanical loading*. Clin Orthop Relat Res, 1999(367 Suppl): p. S356-70.
13. Banes, A.J., et al., *Mechanical load stimulates expression of novel genes in vivo and in vitro in avian flexor tendon cells*. Osteoarthritis Cartilage, 1999. **7**(1): p. 141-53.
14. McNeilly, C.M., et al., *Tendon cells in vivo form a three dimensional network of cell processes linked by gap junctions*. J Anat, 1996. **189** (Pt **3**): p. 593-600.
15. Komanduri, M., C.S. Phillips, and D.P. Mass, *Tensile strength of flexor tendon repairs in a dynamic cadaver model*. J Hand Surg Am, 1996. **21**(4): p. 605-11.
16. Savage, R. and G. Risitano, *Flexor Tendon Repair Using a 6 Strand Method of Repair and Early Active Mobilization*. Journal of Hand Surgery-British and European Volume, 1989. **14B**(4): p. 396-399.
17. Silfverskiold, K.L. and C.H. Andersson, *Two new methods of tendon repair: an in vitro evaluation of tensile strength and gap formation*. J Hand Surg Am, 1993. **18**(1): p. 58-65.
18. Pruitt, D.L., P.R. Manske, and B. Fink, *Cyclic stress analysis of flexor tendon repair*. J Hand Surg Am, 1991. **16**(4): p. 701-7.
19. Strickland, J.W., *Flexor Tendon Injuries: I. Foundations of Treatment*. J Am Acad Orthop Surg, 1995. **3**(1): p. 44-54.
20. Koob, T.J., *"Collagen Fixation"*. Encyclopedia of Biomaterials and Biomedical Engineering, 2004. **1**(1): p. 335-347.
21. Fisher, J.P., *Tissue Engineering*. 2007, CRC Press/Taylor & Francis Group: Boca Raton.
22. Mendes, D.G., et al., *Ligament and tendon substitution with composite carbon fiber strands*. J Biomed Mater Res, 1986. **20**(6): p. 699-708.
23. Hunter, J.M., et al., *Active tendon implants in flexor tendon reconstruction*. J Hand Surg Am, 1988. **13**(6): p. 849-59.
24. Fujikawa, K., et al., *Reconstruction of the extensor apparatus of the knee with the Leeds-Keio ligament*. J Bone Joint Surg Br, 1994. **76**(2): p. 200-3.
25. Woo, S.L., et al., *Tissue engineering of ligament and tendon healing*. Clin Orthop Relat Res, 1999(367 Suppl): p. S312-23.

26. Anderson, D.G., et al., *Biomaterial microarrays: rapid, microscale screening of polymer-cell interaction*. *Biomaterials*, 2005. **26**(23): p. 4892-7.
27. Liu, W.F., Chen, C.S., *Engineering biomaterials to control cell function*. *Materials Today* 2005. **8**(12): p. 28-35.
28. Jacot, J.G., A.D. McCulloch, and J.H. Omens, *Substrate stiffness affects the functional maturation of neonatal rat ventricular myocytes*. *Biophys J*, 2008. **95**(7): p. 3479-87.
29. Paszek, M.J., et al., *Tensional homeostasis and the malignant phenotype*. *Cancer Cell*, 2005. **8**(3): p. 241-54.
30. Awad, H.A., et al., *Autologous mesenchymal stem cell-mediated repair of tendon*. *Tissue Eng*, 1999. **5**(3): p. 267-77.
31. Young, R.G., et al., *Use of mesenchymal stem cells in a collagen matrix for Achilles tendon repair*. *Journal of Orthopaedic Research*, 1998. **16**(4): p. 406-413.
32. Gartner, L.P. and J.L. Hiatt, *Color Textbook of Histology*. 3rd ed. 2007, Philadelphia: Saunders Elsevier.
33. Fedorczyk, J.M., *Tendinopathies of the elbow, wrist, and hand: histopathology and clinical considerations*. *J Hand Ther*, 2012. **25**(2): p. 191-200; quiz 201.
34. Koob, T.J. and A.P. Summers, *Tendon--bridging the gap*. *Comp Biochem Physiol A Mol Integr Physiol*, 2002. **133**(4): p. 905-9.
35. Eyre, D.R., M.A. Paz, and P.M. Gallop, *Cross-linking in collagen and elastin*. *Annu Rev Biochem*, 1984. **53**: p. 717-48.
36. Rault, I., et al., *Evaluation of different chemical methods for cross-linking collagen gel, films and sponges*. *Journal of Materials Science: Materials in Medicine*, 1996. **7**(4): p. 215-221.
37. Bigi, A., et al., *Mechanical and thermal properties of gelatin films at different degrees of glutaraldehyde crosslinking*. *Biomaterials*, 2001. **22**(8): p. 763-8.
38. Olde Damink, L.H., et al., *Cross-linking of dermal sheep collagen using a water-soluble carbodiimide*. *Biomaterials*, 1996. **17**(8): p. 765-73.
39. Lu, J.M., et al., *Molecular mechanisms and clinical applications of nordihydroguaiaretic acid (NDGA) and its derivatives: an update*. *Med Sci Monit*, 2010. **16**(5): p. RA93-100.

40. Koob, T.J. and D.J. Hernandez, *Mechanical and thermal properties of novel polymerized NDGA-gelatin hydrogels*. *Biomaterials*, 2003. **24**(7): p. 1285-92.
41. Koob, T.J. and D.J. Hernandez, *Material properties of polymerized NDGA-collagen composite fibers: development of biologically based tendon constructs*. *Biomaterials*, 2002. **23**(1): p. 203-12.
42. Moussy, Y., et al., *Transport characteristics of a novel local drug delivery system using nordihydroguaiaretic acid (NDGA)-polymerized collagen fibers*. *Biotechnol Prog*, 2007. **23**(4): p. 990-4.
43. Lu, X., et al., *Crosslinking effect of Nordihydroguaiaretic acid (NDGA) on decellularized heart valve scaffold for tissue engineering*. *J Mater Sci Mater Med*, 2010. **21**(2): p. 473-80.
44. Zhu, C., G. Bao, and N. Wang, *Cell mechanics: mechanical response, cell adhesion, and molecular deformation*. *Annu Rev Biomed Eng*, 2000. **2**: p. 189-226.
45. Garcia, A.J. and N.D. Gallant, *Stick and grip: measurement systems and quantitative analyses of integrin-mediated cell adhesion strength*. *Cell Biochem Biophys*, 2003. **39**(1): p. 61-73.
46. Schmidt, C.E., et al., *Integrin-cytoskeletal interactions in migrating fibroblasts are dynamic, asymmetric, and regulated*. *J Cell Biol*, 1993. **123**(4): p. 977-91.
47. Christ, K.V. and K.T. Turner, *Methods To Measure the Strength of Cell Adhesion to Substrates*. *Journal of Adhesion Science and Technology* 2010. **24**: p. 2027-2058.
48. Chu, L., et al., *Centrifugation assay of IgE-mediated cell-adhesion to antigen-coated gels*. *AIChE Journal*, 1994. **40**: p. 692-703.
49. Reyes, C.D. and A.J. Garcia, *A centrifugation cell adhesion assay for high-throughput screening of biomaterial surfaces*. *Journal of Biomedical Materials Research Part A*, 2003. **67A**(1): p. 328-333.
50. Giacomello, E., et al., *Centrifugal assay for fluorescence-based cell adhesion adapted to the analysis of ex vivo cells and capable of determining relative binding strengths*. *Biotechniques*, 1999. **26**(4): p. 758-62, 764-6.
51. McKeever, P.E., *Methods to study pulmonary alveolar macrophage adherence micromanipulation and quantitation*. *J Reticuloendothel Soc*, 1974. **16**(6): p. 313-7.

52. van Kooten, T.G., et al., *Development and use of a parallel-plate flow chamber for studying cellular adhesion to solid surfaces*. Journal of Biomedical Materials Research 1992. **26**(6): p. 725-738.
53. Michael, K.E. and A.J. Garcia, *Cell adhesion strengthening: measurement and analysis*. Methods Cell Biol, 2007. **83**: p. 329-46.
54. Garcia, A.J., F. Huber, and D. Boettiger, *Force required to break alpha5beta1 integrin-fibronectin bonds in intact adherent cells is sensitive to integrin activation state*. J Biol Chem, 1998. **273**(18): p. 10988-93.
55. Garcia, A.J., P. Ducheyne, and D. Boettiger, *Quantification of cell adhesion using a spinning disc device and application to surface-reactive materials*. Biomaterials, 1997. **18**(16): p. 1091-8.
56. Martin, P., *Wound healing--aiming for perfect skin regeneration*. Science, 1997. **276**(5309): p. 75-81.
57. Palecek, S.P., et al., *Integrin dynamics on the tail region of migrating fibroblasts*. J Cell Sci, 1996. **109** (Pt 5): p. 941-52.
58. Brakebusch, C., et al., *Integrins in invasive growth*. J Clin Invest, 2002. **109**(8): p. 999-1006.
59. Laukaitis, C.M., et al., *Differential dynamics of alpha 5 integrin, paxillin, and alpha-actinin during formation and disassembly of adhesions in migrating cells*. J Cell Biol, 2001. **153**(7): p. 1427-40.
60. DiMilla, P.A., K. Barbee, and D.A. Lauffenburger, *Mathematical model for the effects of adhesion and mechanics on cell migration speed*. Biophys J, 1991. **60**(1): p. 15-37.
61. Palecek, S.P., et al., *Integrin-ligand binding properties govern cell migration speed through cell-substratum adhesiveness*. Nature, 1997. **385**(6616): p. 537-40.
62. Benigno, K.A., et al., *Nascent focal adhesions are responsible for the generation of strong propulsive forces in migrating fibroblasts*. J Cell Biol, 2001. **153**(4): p. 881-8.
63. Lampugnani, M.G., *Cell Migration into a Wounded Area In Vitro Adhesion Protein Protocols*, E. Dejana and M. Corada, Editors. 1999, Humana Press. p. 177-182.
64. Yarrow, J.C., et al., *A high-throughput cell migration assay using scratch wound healing, a comparison of image-based readout methods*. BMC Biotechnol, 2004. **4**: p. 21.

65. Keese, C.R., et al., *Electrical wound-healing assay for cells in vitro*. Proc Natl Acad Sci U S A, 2004. **101**(6): p. 1554-9.
66. Pratt, B.M., et al., *Mechanisms of cytoskeletal regulation. Modulation of aortic endothelial cell spectrin by the extracellular matrix*. Am J Pathol, 1984. **117**(3): p. 349-54.
67. Sagnella, S.M., et al., *Human microvascular endothelial cell growth and migration on biomimetic surfactant polymers*. Biomaterials, 2004. **25**(7-8): p. 1249-59.
68. Kondo, H., R. Matsuda, and Y. Yonezawa, *Autonomous migration of human fetal skin fibroblasts into a denuded area in a cell monolayer is mediated by basic fibroblast growth factor and collagen*. In Vitro Cell Dev Biol Anim, 1993. **29A**(12): p. 929-35.
69. Koob, T.J., T.A. Willis, and D.J. Hernandez, *Biocompatibility of NDGA-polymerized collagen fibers. I. Evaluation of cytotoxicity with tendon fibroblasts in vitro*. J Biomed Mater Res, 2001. **56**(1): p. 31-9.
70. Koob, T.J., et al., *Biocompatibility of NDGA-polymerized collagen fibers. II. Attachment, proliferation, and migration of tendon fibroblasts in vitro*. J Biomed Mater Res, 2001. **56**(1): p. 40-8.
71. Wyko NT9100 Profiler. 2009 [cited 2012 05/08/2012]; Available from: <http://www.clean.cise.columbia.edu/equipment/equipmentlist/122-wyko-nt9100-profiler>.
72. Gallant, N.D., K.E. Michael, and A.J. Garcia, *Cell adhesion strengthening: contributions of adhesive area, integrin binding, and focal adhesion assembly*. Mol Biol Cell, 2005. **16**(9): p. 4329-40.
73. Ju, Y.M., et al., *A novel porous collagen scaffold around an implantable biosensor for improving biocompatibility. I. In vitro/in vivo stability of the scaffold and in vitro sensitivity of the glucose sensor with scaffold*. J Biomed Mater Res A, 2008. **87**(1): p. 136-46.
74. Buxboim, A., I.L. Ivanovska, and D.E. Discher, *Matrix elasticity, cytoskeletal forces and physics of the nucleus: how deeply do cells 'feel' outside and in?* J Cell Sci, 2010. **123**(Pt 3): p. 297-308.
75. Buxboim, A., et al., *How deeply cells feel: methods for thin gels*. J Phys Condens Matter, 2010. **22**(19): p. 194116.

76. Grover, C.N., et al., *Crosslinking and composition influence the surface properties, mechanical stiffness and cell reactivity of collagen-based films*. Acta Biomater, 2012.

APPENDICES

Appendix A: Copyright Permissions

A.1 Permission to Use Figure 2

ELSEVIER LICENSE
TERMS AND CONDITIONS

Jun 10, 2012

This is a License Agreement between University of South Florida ("You") and Elsevier ("Elsevier") provided by Copyright Clearance Center ("CCC"). The license consists of your order details, the terms and conditions provided by Elsevier, and the payment terms and conditions.

All payments must be made in full to CCC. For payment instructions, please see information listed at the bottom of this form.

| | |
|--|--|
| Supplier | Elsevier Limited The Boulevard, Langford Lane Kidlington, Oxford, OX5 1GB, UK |
| Registered Company Number | 1982084 |
| Customer name | University of South Florida |
| Customer address | ██████████ ██████████ |
| License number | 2925690911267 |
| License date | Jun 10, 2012 |
| Licensed content publisher | Elsevier |
| Licensed content publication | Journal of Hand Therapy |
| Licensed content title | Tendinopathies of the Elbow, Wrist, and Hand: Histopathology and Clinical Considerations |
| Licensed content author | Jane M. Fedorczyk |
| Licensed content date | April–June 2012 |
| Licensed content volume number | 25 |
| Licensed content issue number | 2 |
| Number of pages | 11 |
| Start Page | 191 |
| End Page | 201 |
| Type of Use | reuse in a thesis/dissertation |
| Portion | figures/tables/illustrations |
| Number of figures/tables/illustrations | 1 |
| Format | both print and electronic |
| Are you the author of this Elsevier article? | No |
| Will you be translating? | No |
| Order reference number | |
| Title of your thesis/dissertation | Cell Adhesion and Migration on NDGA Cross-linked Fibrillar Collagen Matrices for Tendon Tissue Engineering |

Appendix A (Continued)

| | |
|----------------------------------|-------------------|
| Expected completion date | Aug 2012 |
| Estimated size (number of pages) | 100 |
| Elsevier VAT number | GB 494 6272 12 |
| Permissions price | 0.00 USD |
| VAT/Local Sales Tax | 0.0 USD / 0.0 GBP |
| Total | 0.00 USD |

Appendix A (Continued)

A.2 Permission to Use Figure 6


ELSEVIER LICENSE TERMS AND CONDITIONS

May 31, 2012

=====

This is a License Agreement between University of South Florida ("You") and Elsevier ("Elsevier") provided by Copyright Clearance Center ("CCC"). The license consists of your order details, the terms and conditions provided by Elsevier, and the payment terms and conditions.

All payments must be made in full to CCC. For payment instructions, please see information listed at the bottom of this form.

| | |
|--|---|
| Supplier | Elsevier Limited The Boulevard, Langford Lane Kidlington, Oxford, OX5 1GB, UK |
| Registered Company Number | 1982084 |
| Customer name | University of South Florida |
| Customer address |  |
| License number | 2919470168623 |
| License date | May 31, 2012 |
| Licensed content publisher | Elsevier |
| Licensed content publication | Biomaterials |
| Licensed content title | Mechanical and thermal properties of novel polymerized NDGA-gelatin hydrogels |
| Licensed content author | Thomas J. Koob, Daniel J. Hernandez |
| Licensed content date | March 2003 |
| Licensed content volume number | 24 |
| Licensed content issue number | 7 |
| Number of pages | 8 |
| Start Page | 1285 |
| End Page | 1292 |
| Type of Use | reuse in a thesis/dissertation |
| Portion | figures/tables/illustrations |
| Number of figures/tables/illustrations | 1 |
| Format | both print and electronic |

Appendix A (Continued)

| | |
|--|--|
| Are you the author of this Elsevier article? | No |
| Will you be translating? | No |
| Title of your thesis/dissertation | Cell Adhesion and Migration on NDGA Cross-linked Fibrillar Collagen Matrices for Tendon Tissue Engineering |
| Expected completion date | Aug 2012 |
| Estimated size (number of pages) | 100 |
| Elsevier VAT number | GB 494 6272 12 |

ABOUT THE AUTHOR

Ana Ysabel Rioja was born in Lima, Peru. She and her family moved to Tampa, Florida where she attended middle and high school. She received her Bachelor's degree in Chemical Engineering on May 2010 from the University of South Florida (USF), and will be graduating with her Masters degree in Biomedical Engineering on August 2012 from this same institution. During her years at USF, she participated in organizations that promote engineering to K-12 students. She plans to continue her participation with this type of organization at the University of Michigan, where she will be pursuing her doctoral degree in Biomedical Engineering. Her future goals are to have a transformative impact on the treatment of cardiovascular diseases by engineering biomaterials for cardiac regeneration. She hopes to create a degradable and non-immunogenic biomaterial that can be used to regenerate the damaged cardiac muscle tissue by inducing the migration of resident cells from the surrounding tissues. She also plans to create outreach programs that would help students finish their education and inspire them to earn doctoral degrees in their fields of study.